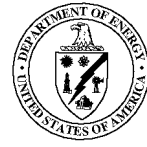

C
S
P

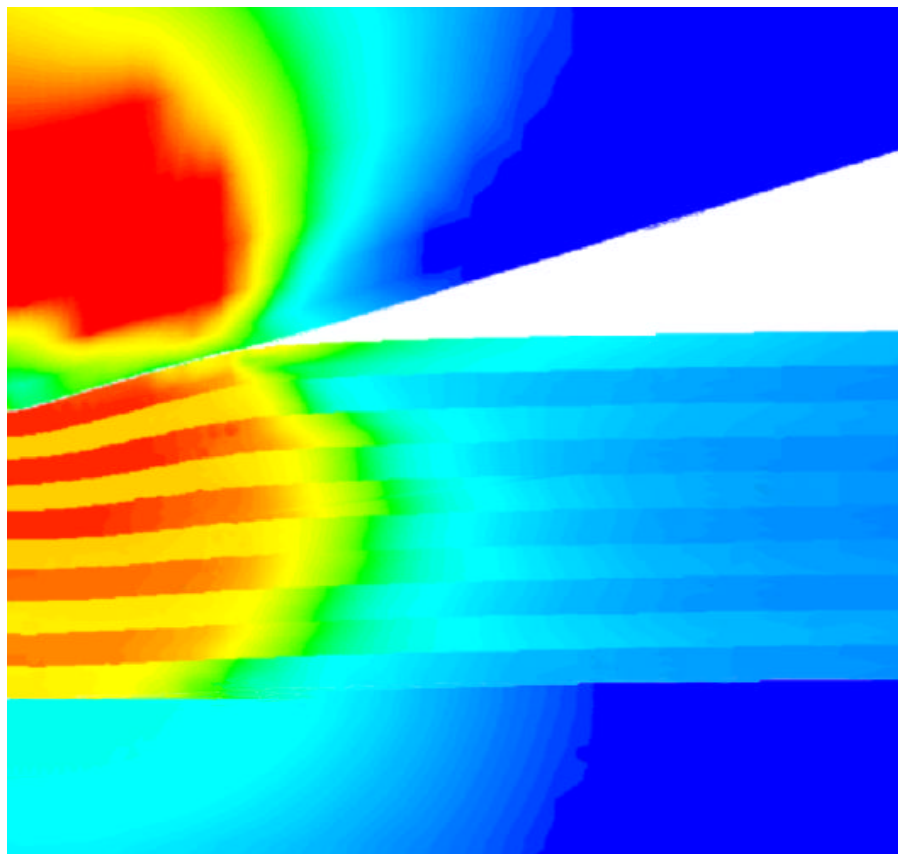
The DOE Center of Excellence for the
Synthesis and Processing
of Advanced Materials



BASIC ENERGY SCIENCES
DIVISION OF MATERIALS SCIENCES

Member Laboratories: *Ames Laboratory, Argonne National Laboratory, Brookhaven National Laboratory, Idaho National Engineering and Environmental Laboratory, University of Illinois Frederick Seitz Materials Research Laboratory, Lawrence Berkeley National Laboratory, Lawrence Livermore National Laboratory, Los Alamos National Laboratory, National Renewable Energy Laboratory, Oak Ridge National Laboratory, Pacific Northwest National Laboratory, Sandia National Laboratories*

Research Briefs



For questions and additional information contact:

George A. Samara
Sandia National Laboratories/NM
Phone: (505) 844-6653
Fax: (505) 844-4045
E-mail: gasamar@sandia.gov

C
S
P

The DOE **C**enter of Excellence for the
Synthesis and **P**rocessing
of Advanced Materials



BASIC ENERGY SCIENCES
DIVISION OF MATERIALS SCIENCES

Research Briefs

February 1998

TABLE OF CONTENTS

PREFACE	4
THE CENTER'S MEMBER LABORATORIES	6
CENTER PROJECTS AND THEIR COORDINATORS	7
EXECUTIVE SUMMARY.....	8

Research Briefs

MECHANICALLY RELIABLE SURFACE OXIDES FOR HIGH-TEMPERATURE CORROSION RESISTANCE.....	14
• Comparison of Measured and Modeled Stresses Near the Edge of Alumina Scales	14
• Sulfur Segregation to Deposited Al ₂ O ₃ Film-Alloy Interfaces.....	16
• Microstructural Characterization of Reactive Element Segregation in Alumina Scales as Related to Oxidation Behavior	18
METAL FORMING	20
• New Scaling Relationships for Dislocation Microstructures in Deformed Metals.....	20
• Measurement of Initial and Hot Deformation Textures in an Aluminum Alloy.....	22
• Grain Refinement for Superplasticity in Al-Mg-Mn-Sc Alloys.....	24
PROCESSING FOR SURFACE HARDNESS.....	26
• Coatings for Reduced Friction and Wear in Micro-Electromechanical Systems	26
• Finite-Element Modeling of Nanoindentation for Evaluating Mechanical Properties of Thin Films and Implanted Layers.....	28
• Improved Process for Depositing Thick, Adherent Films of Cubic Boron Nitride.....	30

MICROSTRUCTURAL ENGINEERING WITH POLYMERS	32
• Molecular Engineering of Structured Polymer-Polymer Nanocomposites	32
• Conformation and Dynamics of Structure-Directing Molecules in Tailored Composites	34
• Modeling Properties of Polymer Blends	36
MATERIALS JOINING	38
• A Novel Approach to Understanding Weld Pool Solidification Using Metal-Analogue Systems	38
• Joining of SiC-Based Ceramics for Elevated Temperature Applications	40
• Improved Properties of Joints Between SiC/SiC Composites from Further Development of Low Temperature Bonding Process	42
TAILORED MICROSTRUCTURES IN HARD MAGNETS.....	44
• Nanocrystalline Composite Coercive Magnet Powder	44
• Epitaxial Exchange-Spring Magnets.....	46
• Magnetic Anisotropy and its Microstructural Origins: Advances in Electron-Optical Characterization	48
HIGH EFFICIENCY PHOTOVOLTAICS.....	50
• Light-Induced Metastability in Hydrogenated Amorphous Silicon.....	50
• Interfacial Microstructure in CdTe/CdS Heterojunction Solar Cells.....	52
• Dopant effects on Silicon Selective Nucleation and Solid Phase Epitaxy	54
DESIGN AND SYNTHESIS OF ULTRAHIGH-TEMPERATURE INTERMETALLICS	56
• Synthesis and Properties of Mo ₅ Si ₃ Single Crystals	56
• Bonding Mechanism and Elastic Properties of Mo ₅ Si ₃	58
• Superplastic Formability of Advanced Silicides	60

PREFACE

This publication, *Research Briefs*, is designed to inform present and potential customers and partners of the **DOE Center of Excellence for the Synthesis and Processing of Advanced Materials** about significant advances resulting from Center-coordinated research. The format for *Research Briefs* is an easy-to-read, not highly technical, concise presentation of the accomplishments. Each *Brief* provides a statement of the motivation for the research followed by a description of the accomplishment and its significance.

The Center is a distributed center for promoting coordinated, cooperative research partnerships related to the synthesis and processing of advanced materials. It was established by the Department of Energy's Division of Materials Sciences, Office of Basic Energy Sciences and the DOE Laboratories in recognition of the enabling role of materials synthesis and processing to numerous materials fabrication- and manufacturing-intensive technologies. The participants include investigators from 12 DOE national laboratories, universities and the private sector. The Center has a technology perspective provided by a Technology Steering Group.

By bringing together synergistic activities and capabilities in selected focus areas of materials synthesis and processing, the Center's goal is to be a vehicle for providing added value and making impact. The Center is also allowing better coordinated strategic planning by the Division of Materials Sciences and the Laboratories and faster response time to special needs and opportunities. Additionally, the Center strives to be a model of R and D integration within the Department of Energy as well as a model of cooperation among the participating institutions.

The overall objective of the Center is,

To enhance the science and engineering of materials synthesis and processing in order to meet the programmatic needs of the Department of Energy and to facilitate the technological exploitation of materials.

Synthesis and processing (S&P) are those essential elements of Materials Science and Engineering (MS&E) that deal with (1) the assembly of atoms or molecules to form materials, (2) the manipulation and control of the structure at all levels from the atomic to the macroscopic scale, and (3) the development of processes to produce materials for specific applications. Clearly, S&P

represent a large area of MS&E that spans the range from fundamental research to technology. The goal of basic research in this area ranges from the creation of new materials and the improvement of the properties of known materials, to the understanding of such phenomena as diffusion, crystal growth, sintering, phase transitions, etc., in relation to S&P. On the applied side, the goal of S&P is to translate scientific results into useful materials by developing processes capable of producing high quality cost-effective products.

The technical emphasis of the Center has been on eight focused multilaboratory projects which draw on the complementary strengths of the member institutions in their ongoing research programs. These projects were selected on the basis of the following criteria:

- scientific excellence
- clear relationship to energy technologies
- involvement of several laboratories
- existing or potential partnerships with DOE Technologies-funded programs
- existing or potential "in-kind" partnerships with industry

Each Project is coordinated by a knowledgeable representative from one of the participating laboratories. The Projects and their Coordinators are listed in the accompanying table. In this issue of *Research Briefs* we have selected a few accomplishments from each of the Projects. An Executive Summary provides highlights of these accomplishments organized by Project. Readers are encouraged to contact any of the Coordinators for information about the Center and its accomplishments.

George A. Samara
February 1998

THE CENTER'S MEMBER LABORATORIES

The member laboratories of the Center are:

- Ames Laboratory (Ames)
- Argonne National Laboratory (ANL)
- Brookhaven National Laboratory (BNL)
- Idaho National Engineering and Environmental Laboratory (INEEL)
- University of Illinois Frederick Seitz Materials Research Laboratory (UI/MRL)
- Lawrence Berkeley National Laboratory (LBNL)
- Lawrence Livermore National Laboratory (LLNL)
- Los Alamos National Laboratory (LANL)
- National Renewable Energy Laboratory (NREL)
- Oak Ridge National Laboratory (ORNL)
- Pacific Northwest National Laboratory (PNNL)
- Sandia National Laboratories (SNL)

CENTER PROJECTS AND THEIR COORDINATORS

PROJECT	COORDINATOR(S)
---------	----------------

Metal Forming	Michael Kassner (Oregon State) Phone: (541) 737-7023 FAX: (541) 737-2600 E-mail: kassner@engr.orst.edu
Materials Joining	R. Bruce Thompson (Ames) Phone: (515) 294-9649 FAX: (515) 294-4456 E-mail: thompsonrb@ameslab.gov
Microstructural Engineering with Polymers	Gregory J. Exarhos (PNNL) Phone: (509) 375-2440 FAX: (509) 375-2186 E-mail: gj_exarhos@pnl.gov
Tailored Microstructures in Hard Magnets	Bob Dunlap (ANL) Phone: (708) 252-4925 FAX: (708) 252-4798 E-mail: bddunlap@anl.gov
Processing for Surface Hardness	James B. Roberto (ORNL) Phone: (423) 576-0227 FAX: (423) 574-4143 E-mail: jlr@ornl.gov
Mechanically Reliable Surface Oxides for High-Temperature Corrosion Resistance	Linda L. Horton (ORNL) Phone: (423) 574-5081 FAX: (423) 574-7659 E-mail: hortonll@mail60.ms.ornl.gov
High Efficiency Photovoltaics	Satyen Deb (NREL) Phone: (303) 384-6405 FAX: (303) 384-6481 E-mail: satyen_deb@nrel.gov
Design and Synthesis of Ultrahigh-Temperature Intermetallics	Roddie R. Judkins (ORNL) Phone: (423) 574-4572 FAX: (423) 574-5812 E-mail: judkinsrr@ornl.gov
	and
	R. Bruce Thompson (Ames) Phone: (515) 294-9649 Fax: (515) 294-4456 E-mail: gasamar@sandia.gov
Overall Center Coordinator	George A. Samara (SNL/NM) Phone: (505) 844-6653 FAX: (505) 844-4045 E-mail: gasamar@sandia.gov

EXECUTIVE SUMMARY

The *Research Briefs* presented in this publication are intended to inform the Center's present and potential customers and partners about significant advances resulting from Center-coordinated research. Selected accomplishments from each of the Center's focused projects are presented. This Executive Summary states the overall objective of each project followed by highlights of the accomplishments presented later in more detail.

Mechanically Reliable Surface Oxides for High-Temperature Corrosion Resistance

Objective

Generate the knowledge required to establish a scientific basis for the design and synthesis of improved (slow growing, adherent, sound) protective oxide coatings and scales on high temperature materials without compromising the requisite bulk material properties.

Highlights

- To better understand the mechanisms that lead to scale failure, we have measured the stress profiles near scale edges that develop during cooling from oxidation temperatures in Al_2O_3 scales and compared the results to finite element, continuum model predictions. The good agreement between results provides confidence in the modeling which produces detailed information necessary for improved understanding and design.
- It has been found that the high temperature segregation of sulfur from a Fe-28Al-5Cr (at.%) alloy to the interface with plasma-deposited Al_2O_3 is controlled by the availability of interfacial binding sites, rather than by its bulk diffusion rate - a finding that is important for understanding and controlling the deleterious influence of sulfur on the adhesion of scales to metal substrates.
- Electron microscopy studies of the segregation of reactive ions at Al_2O_3 - metal interfaces and Al_2O_3 grain boundaries are defining the role of substrate compositional manipulation in impurity segregation, scale and interfacial structure and scale adhesion.

Metal Forming

Objective

Develop a scientific understanding of the phenomena relating to the forming of aluminum alloys for industrial (especially automotive) applications.

Highlights

- We have shown that general scaling relationships do exist which control the dislocation structure as a function of plastic deformation for different metals, different deformation modes and different plastic strains.
- We have developed techniques for measuring initial and hot deformation textures and applied them to the study of a 5182 aluminum alloy. The results give indications for the occurrence of dynamic recrystallization in the deformation process.
- By manipulating the microstructure through an understanding of the role of precipitates in the recrystallization process, we have demonstrated high superplasticity (deformation up to 600% at a strain rate of $1 \times 10^{-4} \text{ s}^{-1}$ and >300% even at $1 \times 10^{-2} \text{ s}^{-1}$) in a relatively low cost Al-Mg alloy similar to the commercial 5083 alloy.

Processing for Surface Hardness

Objective

Understand the critical synthesis and processing issues which limit the use of plasma-based processing for surface hardness and use this understanding to improve the hardness of thin films and coatings.

Highlights

- Diamond-like carbon coating of Ni substrates has led to dramatic improvement in friction and wear compared to uncoated parts under representative MEMS operating conditions.
- Finite-element modeling of experimental nanoindentation results has led to the determination of the yield strength and Young's modulus of thin films and of ion-implanted layers. These mechanical properties allow determination of the intrinsic hardness of the films and layers.
- Using a new high-temperature, low-energy ion-assisted process, thick, adherent films of cubic boron nitride (cBN) have been grown on Si. Nanoindentation measurements combined with finite-element modeling have yielded the first accurate determination of the mechanical properties of the films.

Microstructural Engineering with Polymers

Objective

Develop and implement novel processing methods which direct the evolution of hierarchical microstructures in composites, impart multifunctionality, and induce property changes through blending of components at the molecular level.

Highlights

- We have synthesized polymeric materials containing three-dimensional ordered pore nanostructures from self-assembling monomeric precursors.
- ^{13}C NMR measurements have provided new insights into the conformations and dynamics of structure-directing surfactant molecules in layered-clay/surfactant mixtures. Based on such measurements, appropriate surfactants can be selected to achieve tailored properties in composites.
- Using the off-lattice Polymer Reference Interaction Site Model (PRISM), we have demonstrated that the structural parameters (bond lengths, bond angles, torsion angles, and halogen separations in both the gauche and trans conformations) of small monomeric analogues accurately determine the packing architecture of saturated hydrocarbon polymers (polyolefins) and their halogenated derivatives.

Materials Joining

Objective

Improve the reliability of the processes used to join materials into more complex structures serving a variety of energy-related functions.

Highlights

- We have developed a transparent welding analogue to opaque metallic systems which has allowed the first quantitative study of the complex dynamics of weld pool shape, defect nucleation and growth, and melting as functions of composition, power input and welding rate.
- A pressureless, high-temperature, liquid silicon capillary infiltration process for SiC-SiC joining has yielded high strength joints for temperatures up to $\sim 1200^\circ\text{C}$. The process is suitable for in-field component fabrication and repair.
- Substantial improvement in the high-temperature strength of SiC-SiC joints produced by a pressureless, relatively low temperature process has been achieved by controlling the Al-to-Si ratio in the Al-Si alloy powder used in the simple process which can be used in the field.

Tailored Microstructures in Hard Magnets

Objective

Improve hard magnets by understanding, in terms of the microstructures achieved, the magnetic and mechanical properties of materials produced by a number of synthesis and processing approaches.

Highlights

- We have developed a metallurgical approach toward alloying in the Nd-Fe-B-Ti-C system which allowed the formation of homogeneous, fine-grained, high-coercivity magnetic powders by gas atomization techniques.
- We have designed and studied "exchange-spring magnets" consisting of exchange-coupled bilayers of hard-(SmCo) and soft-(Fe or Co) magnetic phases. Experimental results and model calculations indicate that very large values of the maximum energy product $(BH)_{\max}$ are attainable in exchange-spring structures where the layer thicknesses are on the nanometer length scale.
- High resolution electron microscopy investigations of SmCo films have revealed the presence of atomic-scale defects due to local compositional fluctuations which could explain the high in-plane anisotropies and large coercivity of these films.

High Efficiency Photovoltaics

Objective

Generate advances in scientific understanding that will impact the efficiency, cost and reliability of thin film photovoltaics cells by addressing short- and long-term basic research issues..

Highlights

- A new model for light-induced metastability in hydrogenated amorphous silicon (a-Si:H), the so-called Staebler-Wronski effect responsible for the degradation of a-Si:H solar cells, has been proposed. Molecular dynamic simulations have revealed several atomic configurations that satisfy the model.
- We have demonstrated that x-rays from synchrotron radiation allow a non-destructive and element-specific means for determining interfacial roughness, correlation lengths of thickness fluctuations, elemental density profiles and the local environment of specific atoms in heterojunction solar cells.
- A combined experimental and theoretical approach is being used to elucidate the interactions of dopants, point defects and the amorphous-crystal interface in Si in order to identify the microscopic mechanisms underlying Si solid state epitaxy and thereby to define synthesis routes for producing large-grain poly Si.

Design and Synthesis of Ultrahigh-Temperature Intermetallics

Objective

The objective of this Project is to generate the knowledge required to establish a scientific basis for the processing and design of transition-metal silicides with improved metallurgical and mechanical properties at ambient and high temperatures. Its ultimate goal is to develop scientific principles to design new-generation materials based on silicides for structural applications at temperature at and above 1400°C.

Highlights

- High quality single crystals of Mo_5Si_3 were produced and their orientation-dependent Young's moduli, shear moduli and thermal expansion coefficients were determined. Samples and data were provided to other participants in the Project for theoretical and additional experimental studies. Cumulatively, a detailed base line of the properties of Mo_5Si_3 is being established.
- First-principles calculations have provided an atomic-level understanding of the bonding and anisotropic elastic properties of Mo_5Si_3 . The intrinsic high mechanical strength is a consequence of multi-centered covalent bonds and the strong anisotropy in the thermal expansion results from the anisotropy in lattice anharmonicity.
- Investigations of the microstructure of high temperature, creep deformed single crystal and polycrystalline samples of molybdenum silicides have yielded new insights into the dislocation structure and plasticity of these materials. The addition of a second soft phase appears to be necessary for the promotion of plasticity in Mo_5Si_3 .

Comparison of Measured and Modeled Stresses Near the Edge of Alumina Scales

J. K. Wright and R. L. Williamson, *Idaho National Engineering and Environmental Laboratory*
D. M. Rensch, M. Grimsditch, and B. W. Veal, *Argonne National Laboratory*
R. M. Cannon, *Lawrence Berkeley Laboratory*

Motivation Protective oxide scales often fail prematurely by cracking or spalling at corners. The driving force for these failures is the stress that develops within the scale, primarily in response to the thermal expansion mismatch between the oxide and the substrate during cooling from the processing or service temperature. Therefore, it is important to obtain reliable methods for measuring and understanding stresses in these scales. The objectives of our current efforts are to gain confidence in both the ruby luminescence stress measurement and finite-element modeling (FEM) techniques to better understand surface oxide failure and ultimately to provide criteria for design of more adherent oxides.

Accomplishment The stresses in Al_2O_3 scales that develop during cooling from the oxidation temperature were calculated and compared to measured values. Hydrostatic stresses were measured using the ruby luminescence technique at room temperature to examine the scales formed on oxidized alumina-forming alloys. High spatial resolution of about $2\ \mu\text{m}$ permitted investigation of the stress profiles near scale edges (the intersection of two flat surfaces). Finite element continuum models were used to compute the residual stress and strain fields that develop during cooling. Agreement of computed results with the measured data is very good; both the shapes of the curves and the stress magnitudes are similar.

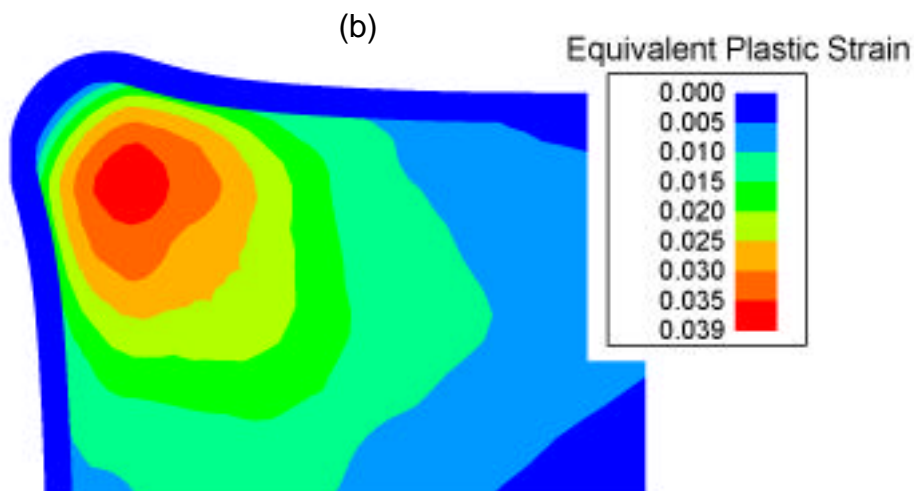
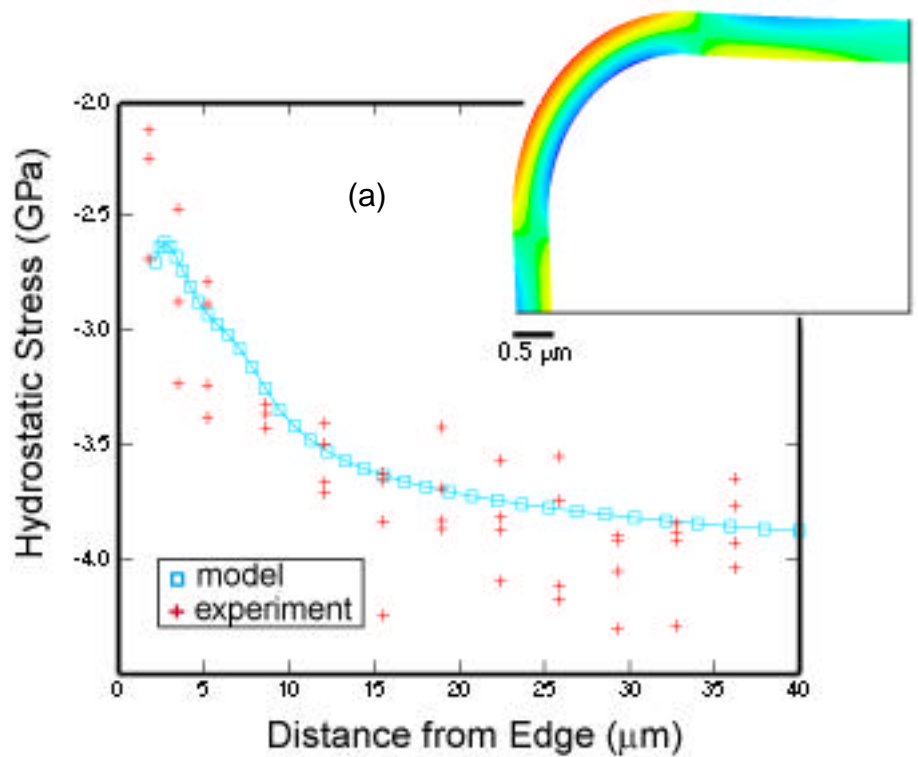
Significance The finite-element modeling (FEM) has proven useful in identifying potential surface oxide failure mechanisms. For example, FEM results indicate that a large tensile stress acts across the interface at the edge regions. Thus, these locations are likely to be sites where delamination can initiate if these stresses are sufficient to initiate growth or coalescence of the smaller flaws that tend to form during oxidation.

Furthermore, substrate plasticity results in bending stresses in the corner region that can be sufficient to cause the scales to crack at the outer surface. The region of highest plastic strain beneath the corner also has a high degree of triaxial tensile stress, which could, in some instances, be a source for cavitation in the metal. These results have significant implications for cases of substrates with low yield stresses, such as model studies using pure metals, many bond coats, and structural alloys operating at very high temperatures.

Ruby luminescence is well suited for measuring stresses in Al_2O_3 . However, it does not measure all the independent stress components and, typically, measurements are spatially averaged over the entire thickness from which the signal is collected. The averaging results in a lower measured stress than is present locally. The technique is thus limited in its ability to predict specific failure locations and to measure stress gradients through the scale thickness. The FEM analysis, on the other hand, provides detailed information about all stress and strain components and gradients and is very useful in providing an increased understanding of the complex mechanical response during cooling. However, the results must be verified experimentally (using certain simplifications and assumptions regarding geometry and material properties). The ruby luminescence and FEM methods thus work well in concert. The measurements provide verification of, and confidence in, the modeling, and, in turn, the modeling produces the detailed information necessary for improved understanding, failure prediction, and design improvements.

Research sponsored by the Division of Materials Sciences Office of Basic Energy Sciences and the Office of Fossil Energy, U. S. Department of Energy.

Contact: Jill Wright, Idaho National Engineering and Environmental Laboratory
Phone: (208) 526-9723 Fax: (208) 526-0690 E-mail: jk3@inel.gov



Hydrostatic stresses in a uniform external Al_2O_3 scale on a Fe_3Al substrate with a radius of curvature of $2 \mu\text{m}$ were modeled and measured. Although excellent agreement was found (a), stress gradients and regions of high local stresses near the scale edges (inset) are not apparent from the measurements alone. Local substrate plasticity (b) results in significant bending in this region (shown magnified 5x) which could lead to cracking at the outer surface of the scale or cavitation in the alloy.

Sulfur Segregation to Deposited Al₂O₃ Film-Alloy Interfaces

P. Y. Hou and I. G. Brown, *Lawrence Berkeley National Laboratory*
K. Prübner and K. B. Alexander, *Oak Ridge National Laboratory*

Motivation Sulfur is not only a common impurity in commercial alloys, but also a strong segregant to surfaces and internal interfaces such as grain boundaries. However, it is not known whether similar segregation would occur at an oxide-metal interface and if the behavior in terms of segregation kinetics and concentration should be comparable.

The detrimental effect of sulfur at alloy grain boundaries has been well documented; it causes embrittlement and weakens the alloy. Likewise, its segregation at an oxide-metal interface could be equally damaging. Oxidation studies of Al₂O₃ scale formed on various alloys have indirectly shown a relationship between scale adherence and the alloy's sulfur content; adherent scales form when the bulk concentration of sulfur in the alloys is less than about 1 ppm. However, fundamental questions exist as to effects of very low levels of interfacial sulfur on scale adherence and as to whether sulfur should segregate to an intact oxide-metal interface.

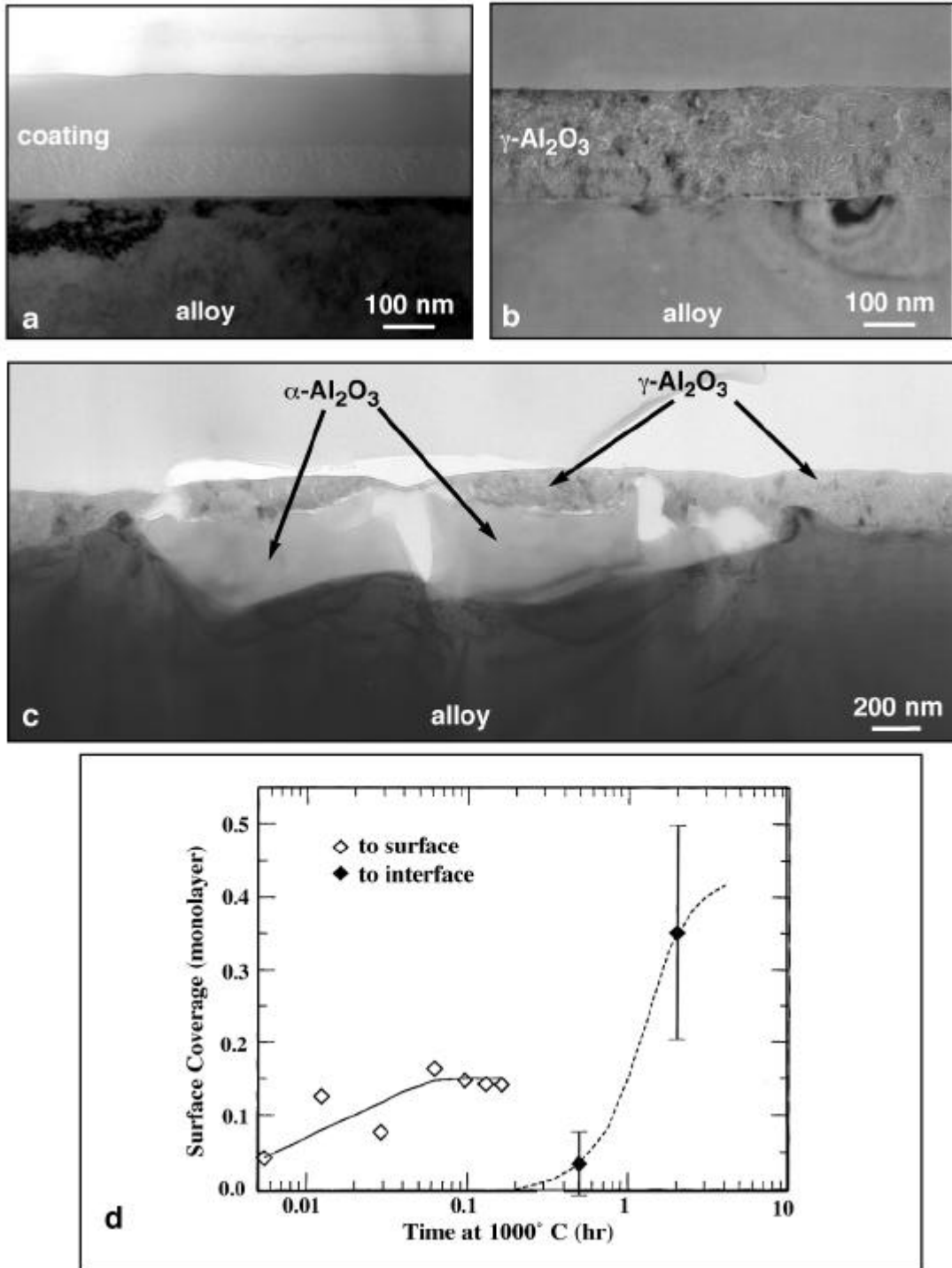
Accomplishment The segregation of indigenous sulfur in an alloy to an existing oxide-alloy interface upon heating was studied using a plasma-deposited Al₂O₃ film on a Fe-28Al-5Cr (at. %) alloy. The as-deposited film was mainly amorphous. Annealing at 1000°C in an inert environment was successfully performed to avoid film growth, yet caused sulfur to slowly segregate to the intact interface. The heat treatment also caused the film to first transform into γ -Al₂O₃ then to α -Al₂O₃. The α -Al₂O₃ grains nucleated at the film-alloy interface, causing significant interface roughening and some

pore formation. The rate of segregation was more than an order of magnitude slower than that to a free surface. The amount of sulfur present at the interface was two times higher than the saturation coverage found on the free surface and it varied with interfacial sites. The variation increased with increasing non-uniformity of the interface structure. From diffusion analysis, using sulfur diffusivity in the alloy, the interfacial segregation rate was also much slower than expected.

Significance The rate of indigenous sulfur segregation to an oxide-metal interface has been studied and directly compared to segregation to a free surface. Two significant differences between surface and interface segregation were found; one was the time to reach saturation and the other was the concentration. From the much slower segregation rate to the interface, the observations of a large variation of the amount of sulfur at different interfacial areas, and the diffusion calculations, it can be concluded that the segregation of sulfur to an oxide-alloy interface is controlled by the availability of interfacial sites, rather than by its bulk diffusion rate. These findings can have significant implications for practices related to desulfurization of alloys for high-temperature service, alloy design, and improvement in the reliability of protective oxide scales.

Research sponsored by the Division of Materials Sciences and the Office of Fossil Energy, U. S. Department of Energy, and the Electric Power Research Institute.

Contact: Peggy Hou, Lawrence Berkeley National Laboratory
Phone: (510) 486-5560 Fax: (510) 486-4995 E-mail: pyhou@lbl.gov



TEM cross-sections of plasma-deposited alumina coatings in the as-deposited state (a) and after heat treatment in He for 0.5 h (b) and for 2 h (c). The heat treatment results in crystallization of the initially amorphous coating and phase transformation from $\gamma\text{-Al}_2\text{O}_3$ to $\alpha\text{-Al}_2\text{O}_3$. Sulfur from the alloy segregates to the metal/ceramic interface during heat treatment (d). The rate of segregation to the interface was much slower than to a free metal surface but the coverage was higher.

Microstructural Characterization of Reactive Element Segregation in Alumina Scales as Related to Oxidation Behavior

K. B. Alexander, K. Prübner, B. A. Pint, and P. F. Tortorelli, *Oak Ridge National Laboratory*

Motivation Thermally grown oxide scales can provide high-temperature oxidation protection if they are slow-growing, sound, and adherent to the substrate. Minor additions of reactive elements (REs) like Y or Zr can decrease oxide growth rates and improve the spallation resistance of the scale. However, while the effects of REs on oxidation behavior have been widely studied, there have been relatively few microstructural studies devoted to relating scale structure, oxide-metal interfacial characteristics, and the reactions associated with indigenous sulfur in the alloy to stress accommodation and oxide adhesion. To this end, transmission electron microscopy (TEM) can provide information on both the microstructure of the scale and the microchemical composition at metal-oxide and oxide-oxide interfaces. Understanding the links among RE doping, interfacial segregation, microstructure, and oxidation performance is the foundation for the development of high-temperature alloys with mechanically reliable oxide scales and, therefore, improved corrosion resistance.

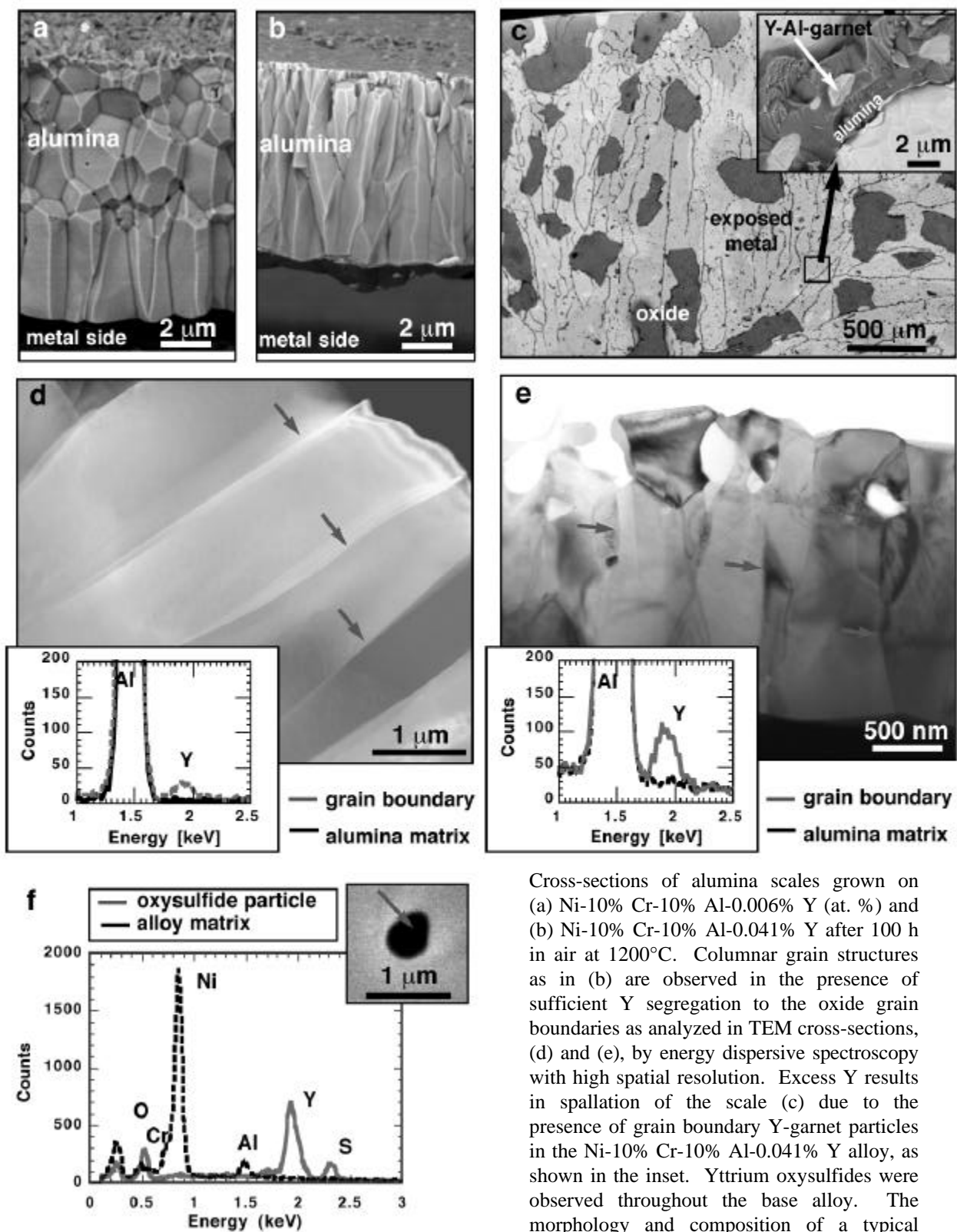
Accomplishment Oxide scales consisting mainly of alumina were grown on various model and developmental alloys (Fe-Al, Fe-Cr-Al, and Ni-Cr-Al, with and without REs) and analyzed in detail by electron microscopy. In general, segregation of the RE ion was observed at the metal-oxide and oxide-oxide interfaces by analytical electron microscopy of thinned scale cross sections. The oxidation performance and scale failure modes were also characterized. The segregation of RE ions to oxide-oxide interfaces tended to alter the morphology of the scale, resulting in a more columnar, slower-growing alumina. However, the presence of RE ion segregants at grain boundaries was not sufficient to ensure improved oxidation performance. For example, while alumina scales on Y-doped Ni-

7% Cr-6.5% Al (at.%) were columnar in nature and well adherent, those on Ni-10% Cr-10% Al spalled despite the RE doping. It was found that the presence of excess RE additions can result in the formation of RE-containing phases at the grain boundaries, which act as sites for enhanced oxidation and, more importantly, for initiation of spallation of the surrounding surface alumina scale. In addition to RE effects on the morphology and composition of the oxide scale, yttrium oxysulfides were observed. The formation of such obviously impacts the ability of indigenous sulfur to segregate to the oxide-metal interface and degrade scale adhesion

Significance While the RE effect has been known for years, there have been relatively few detailed electron microscopy studies despite their value in establishing the necessary structure-performance correlations. To this end, the present observations relate the segregation of RE ions at the oxide-metal and oxide-oxide interfaces with scale microstructure and oxidation performance and are applicable to a wide-variety of alloys and coatings that rely on alumina scales for oxidation protection. The results are of relevance for alumina-forming alloys as well as for thermal barrier coating systems in which failure occurs near or at the interface between a metallic bond coat and its thermally grown alumina layer. This study is helping define the role of substrate compositional manipulations in impurity segregation, scale and interfacial structure and oxide adhesion and should aid in developing more reliable surface oxides for high-temperature corrosion resistance.

Research sponsored by the Division of Materials Sciences, Office of Basic Energy Sciences, the Office of Fossil Energy, and the Advanced Turbine Systems Program in the Office of Industrial Technologies,
U. S. Department of Energy.

Contact: Kathi Alexander, Oak Ridge National Laboratory
Phone: (423) 574-0631 Fax: (423) 574-0641 E-mail: alexanderkb@ornl.gov



Cross-sections of alumina scales grown on (a) Ni-10% Cr-10% Al-0.006% Y (at. %) and (b) Ni-10% Cr-10% Al-0.041% Y after 100 h in air at 1200°C. Columnar grain structures as in (b) are observed in the presence of sufficient Y segregation to the oxide grain boundaries as analyzed in TEM cross-sections, (d) and (e), by energy dispersive spectroscopy with high spatial resolution. Excess Y results in spallation of the scale (c) due to the presence of grain boundary Y-garnet particles in the Ni-10% Cr-10% Al-0.041% Y alloy, as shown in the inset. Yttrium oxysulfides were observed throughout the base alloy. The morphology and composition of a typical particle in Ni-7% Cr-6.5% Al-0.012% Y are shown in (f).

New Scaling Relationships for Dislocation Microstructures in Deformed Metals

D. A. Hughes and A. Godfrey, Sandia National Laboratories, California

D. C. Chrzan, Lawrence Berkeley National Laboratory

Q. Liu and N. Hansen, Risø National Laboratory, Roskilde, Denmark

Motivation Large strain deformations take place in many metal forming processes such as sheet forming, forging, extrusion, and sheet rolling. In all these cases, the plastic deformation creates a subdivision of the initial grains into smaller crystallites separated by dislocation boundaries, and gives rise to a preferred texture. The refinement of the original grain structure by cold working is an ancient technique for imparting superior mechanical properties to the finished product. While dislocation cell formation and grain refinement have been observed and studied extensively, the complexity of the deformed microstructure appeared to defy any quantitative integration of the microstructure into constitutive laws. The discovery of the scaling relationships described below indicates that general relationships do exist which control the evolution of the dislocation structure as a function of the plastic deformation.

Accomplishment A range of metals and alloys have been deformed in different ways to different strain levels, including compressed pure aluminum single crystals, cold rolled aluminum polycrystals, cold rolled nickel polycrystals and high temperature compressed 304L stainless steel. Transmission electron microscopy and convergent beam Kikuchi analysis were performed on the deformed samples to measure the dislocation boundary spacing and misorientation angles. Two different types of dislocation boundaries were identified. Long, continuous dislocation boundaries that have been called geometrically necessary boundaries (GNBs), and smaller scale cell boundaries termed incidental dislocation boundaries (IDBs). For a given material, the average misorientation angle increases while the boundary spacing decreases with increasing

strain for both types of boundaries. In addition, the probability densities of misorientation angles, $P(\theta, \theta_{av})$ (e.g. Fig. 1a), and boundary spacings $P(D, D_{av})$ were calculated for each boundary type from the experimental data. Although each distribution is very different, it was discovered that they can all be scaled according to:

$$P(\theta, \theta_{av}) = \theta_{av} f(\theta/\theta_{av})$$

For the boundary spacings $D(D_{av})$ replaces $\theta(\theta_{av})$ in the equation. For the range over which both parameters scale, $D_{av}\theta_{av}$ is also a constant for a given material. While the scaling applies to all the distributions for the IDBs, Fig. 1b, small deviations are found for the GNBs, as can be seen from Fig. 2. The deviations may be caused by additional factors controlling the GNB misorientation distribution especially at larger strains. The scaling of the misorientation angles breaks down above a strain of $\epsilon = 1$, whereas the scaling relation for the boundary spacings holds to very large strains of $\epsilon = 4.5$ (Fig. 3).

Significance The distributions of misorientation angles for different materials, different deformation modes and different plastic strains are all characterized by a single function with one characteristic parameter, the average misorientation angle. This average value evolves with increasing strain and reflects the microstructural differences due to the material and deformation mode. Additionally, the same scaling relationships can be made for the boundary spacings which are related to the flow stress. The existence of the scaling relationship for the misorientations and spacings indicates that the deformation structure and its evolution are governed by relatively simple laws for the collective properties of dislocation microstructures produced by plastic deformation.

Contact: Darcy A. Hughes, Sandia National Laboratories, California

Phone: (510) 294-2686 Fax: (510) 294-3410 E-mail: darcy_hughes@sandia.gov

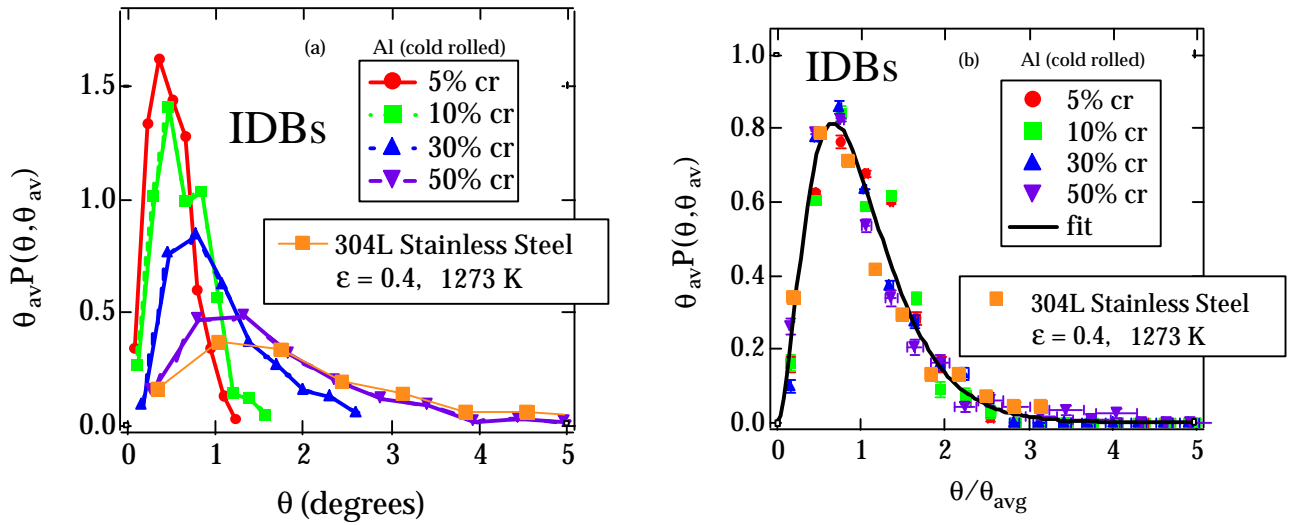


Figure 1 a) Probability densities of the IDB boundary misorientation angles. b) Misorientation angle probability densities scale into one distribution

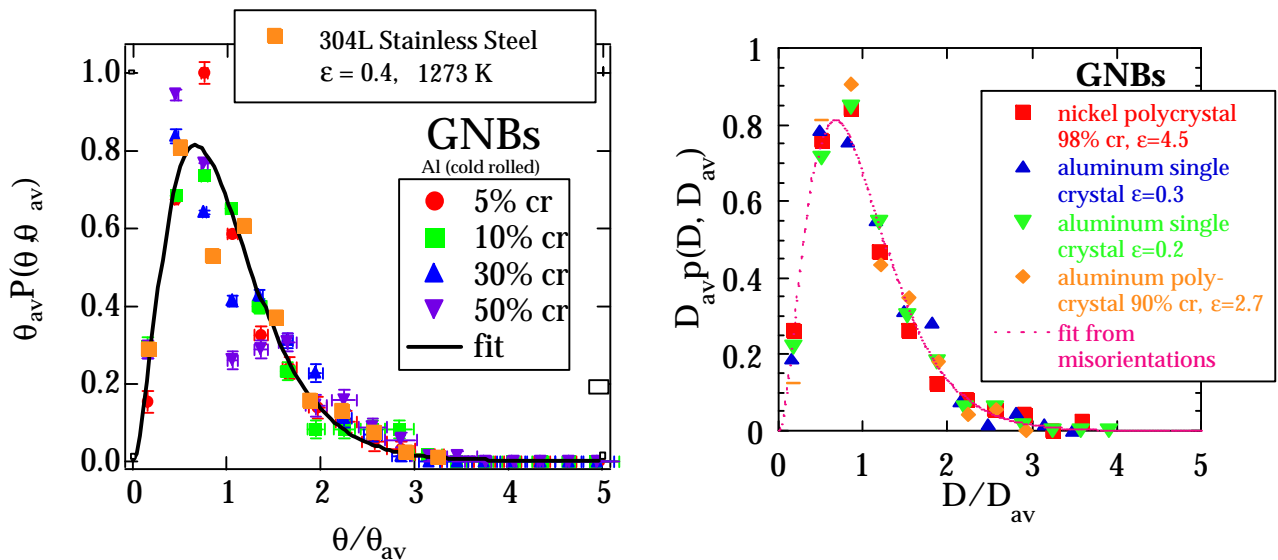


Figure 2. Misorientation angle probability densities of GNBs scale into one distribution.

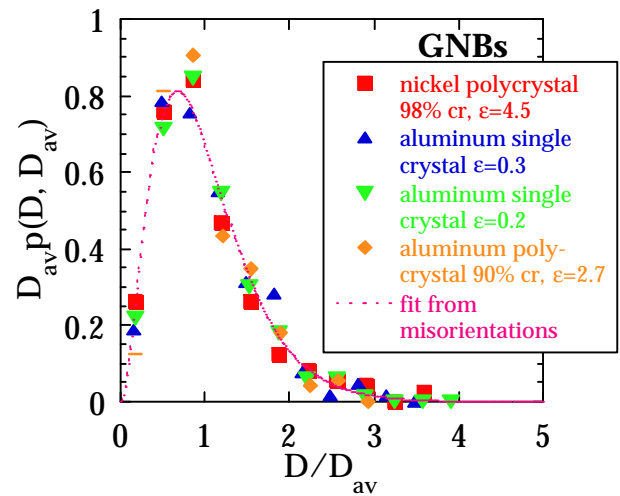


Figure 3. Probability densities of boundary spacings for GNBs scale into one distribution that is similar to that for the misorientation angle.

Measurement of Initial and Hot Deformation Textures in an Aluminum Alloy

M. G. Stout, *Los Alamos National Laboratory*, **R. B. Thompson**, *Ames Laboratory*,
A. Schwartz, *Lawrence Livermore National Laboratory*, **S. R. MacEwen**, *Alcan International*,
B. Radhakrishnan, *Oak Ridge National Laboratory*

Motivation The texture developed during the hot rolling of aluminum plays an important role in its subsequent formability. Texture affects such important metal forming behaviors as work hardening and earing. Our objective is three fold: develop a fundamental understanding of the processes that produce preferred orientations and textures during hot deformation; be able to accurately measure these textures during manufacturing operations; and be able to numerically model and simulate the physical processes that produce the hot deformation textures.

Accomplishment An ultrasonic NDE technique, which can potentially be applied in the field, has been developed for accurately characterizing the texture in aluminum alloys. This technique uses sums and differences in elastic wave velocities to determine orientation coefficients (ODC's), expressed as W_{lmn} , from a harmonic analysis of the material's texture. Because it uses sums and differences, this technique is not sensitive to material alloying content, which alters the absolute wave velocities. Results of this analysis for W_{400} , W_{420} , and W_{440} , measured on our 5182 alloy, have been compared to those from the conventional technique of x-ray diffraction. The agreement between the two techniques is excellent. These ODC's describe a texture that is classically referred to as a "cube" texture. Such a texture is known to be the result of static recrystallization, and it is not surprising that our material has such an initial texture.

We have deformed our material in compression at a variety of temperatures and strain rates, measuring the constitutive response as well as its texture after deformation. There are three physical mechanisms by which the metal

deforms: dynamic strain aging, thermally-activated dislocation recovery, and diffusion-controlled solute drag. We determined that diffusion-controlled solute drag operates in the temperature and strain-rate regime of hot rolling.

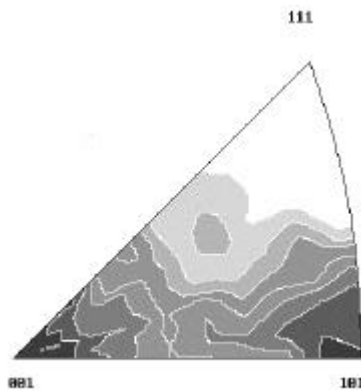
We found that the texture of the compression specimens, deformed in the regime of diffusion-controlled solute drag, had strong cube, (001), and deformation, (101), components (plane normals) parallel to the axis of compression. This is shown in the inverse pole figure taken from material compressed at 550°C and a strain rate of 10^{-3} s^{-1} . Orientation image microscopy (OIM) results confirmed this x-ray observation. One can see two preferred orientations in the OIM micrograph. The red grains have the (101) deformation orientation and the blue grains the (001) recrystallization orientation. One observes instances of blue grain surrounded and nearly surrounded by red grains, as though the (001) orientation is nucleating from the triple points of the deformation orientation. This is what would be expected from static recrystallization. However, these specimens were quenched immediately, in less than 3 seconds, after deformation to a temperature below aluminum's recrystallization temperature. The aluminum should not have had time to statically recrystallize. This is strong indication that dynamic recrystallization is possibly occurring.

Significance Our preliminary results indicate that nonconventional texture development occurs during the hot rolling processes. We are developing the ability to measure these textures in real time during the manufacturing operation. It is important to be able to numerically model and predict this texture development.

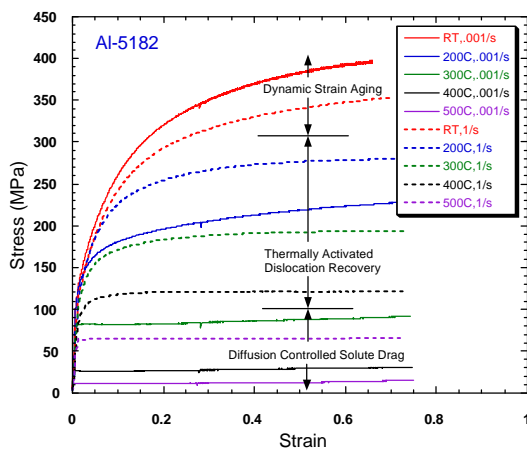
Contact: M. G. Stout, Los Alamos National Laboratory
Phone: (505) 667-6750 Fax: (505) 665-4013 E-mail: mstout@lanl.gov

ODC	ultrasonics Ames	x-ray Los Alamos
W_{400}	5.0	4.0
W_{420}	-0.6	0.21
W_{440}	1.1	0.4

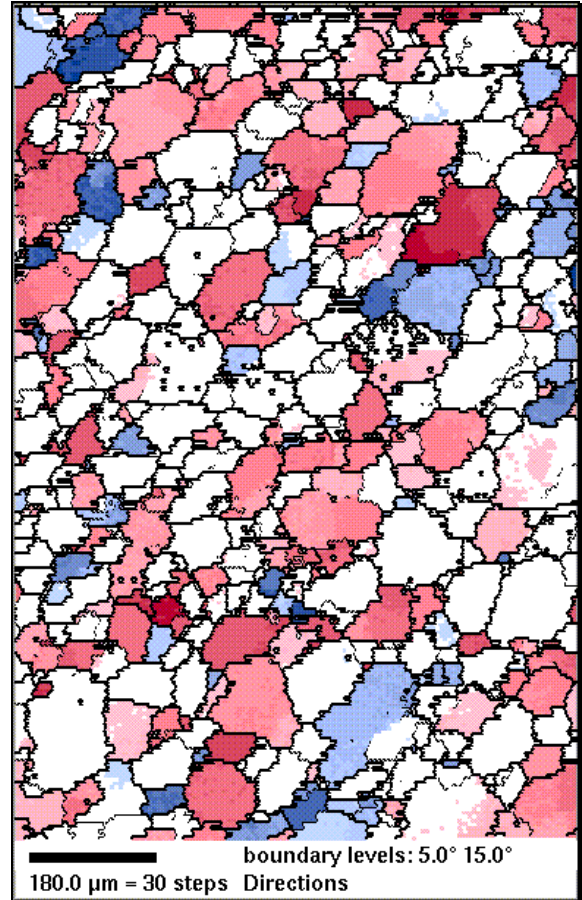
A comparison of ODC measurement results for our 5182 alloy from ultrasonics and x-ray analysis.



Inverse pole figure taken from a compression specimen deformed at 550°C and a strain rate of 10^{-3} s^{-1} to a strain of 0.7. The specimen was quenched immediately after deformation.



Constitutive response of our 5182 aluminum alloy as a function of temperature and strain rate.



Orientation image micrograph of the 550°C compression specimen taken at Lawrence Livermore. The section was taken normal to the compression axis. The red grains represent the (101) deformation orientation, the blue grains a (001) recrystallization orientation. One can see that the (001) orientation is often surrounded or nearly surrounded by the red (101) deformation orientation

Grain Refinement for Superplasticity in Al-Mg-Mn-Sc Alloys

J. S. Vetrano and S. M. Bruemmer, *Pacific Northwest National Laboratory*
L. M. Pawlowski and I. M. Robertson, *University of Illinois*

Motivation Superplasticity, the process by which materials can be made to undergo extremely high plastic deformation, generally requires that the material have a fine grain size. Often the processing required to achieve fine grains is too expensive for high-volume applications such as in the automotive industry. This research seeks to manipulate the recrystallized microstructure in a relatively low-cost Al-4%Mg-1%Mn-0.5%Sc alloy (similar to the commercial alloy 5083 except for the Sc addition) by forming a better understanding of the role of particles in the recrystallization process. This information will then be utilized to optimize the thermomechanical processing and create a fine-grained, superplastic material using industrially relevant techniques.

Accomplishment In-situ heating studies in the transmission electron microscope (TEM) revealed that the recrystallization nuclei in these alloys are primarily micron-sized particles that are produced during casting. Following nucleation, smaller particles can restrict subsequent grain boundary movement and promote a fine-grained microstructure through Zener pinning. This can be seen in the time sequence micrographs of Figure 1 which show a curved grain boundary pinned by a small cluster of Al₆Mn particles (Figure 1a) and the movement of the boundary as it overcomes the pinning force (Figure 1b). Scandium additions create submicron Al₃Sc particles which can be manipulated by heat treatments to form very fine particles that are coherent with the matrix (Figure 2a) or slightly larger particles that are incoherent (Figure 2b). In-situ studies have shown that when the Al₃Sc precipitates are coherent they strongly pin the substructure and restrict the recrystallization process, and when they are larger they effectively pin grain

boundary migration and slow grain growth. By understanding the role of particles on the recrystallization process in these alloys, thermomechanical processing could be designed to tailor the particle size and coherency, and manipulate the final grain structure. A low-temperature heat treatment (300°C/50 hr.) formed coherent Al₃Sc particles and the material was very resistant to recrystallization even at temperatures near the melting point, indicating that nucleation was limited by particles pinning the substructure. The superplastic response for material in this condition was poor. To create incoherent (over-aged) Al₃Sc particles, a 500°C/2 hr. heat treatment was utilized. By a simple cold rolling and recrystallization process used in the commercial aluminum industry, a grain size of 4.4 μm was obtained for this heat treatment. This was achieved by optimizing the balance between grain nucleation and growth. The generation of this fine-grained structure resulted in a material that was highly superplastic; deforming up to 600% at a moderate strain rate of $1 \times 10^{-4} \text{ s}^{-1}$, and more than 300% even at the high strain rate of $1 \times 10^{-2} \text{ s}^{-1}$ (Figure 3). In contrast, the maximum elongation achieved in commercial 5083 is about half that value, even at slow strain rates.

Significance Superplastic deformation can significantly reduce production cost, part count and final weight of a vehicle which translates directly into an overall energy saving. This research shows how material processing for a fine grain size can be tailored by a thorough understanding of the role of particles in the recrystallization process. Collaborative research through the Center's activities will further elucidate the influence of particle size distribution on deformation, recrystallization and grain growth.

Contact: John S. Vetrano, Pacific Northwest National Laboratory
Phone: (509) 372-0724 Fax: (509) 376-6308 E-mail: js_vetrano@pnl.gov

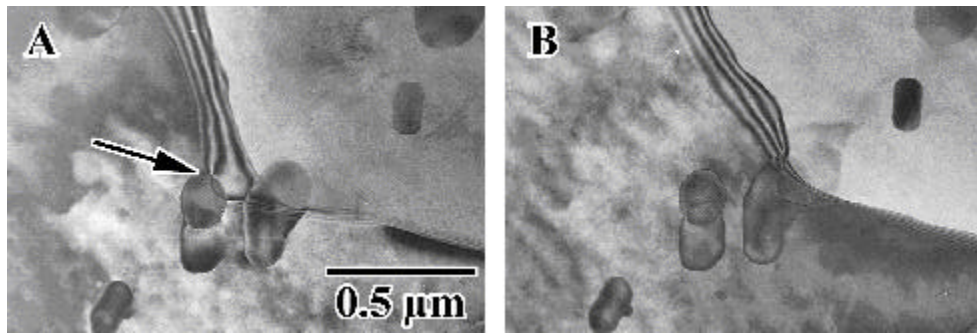


Figure 1. In-situ recrystallization of an Al-Mg-Mn alloy in the TEM showing pinning of the grain boundary by Al_6Mn particles. As the boundary moves from left to right it is pinned by the arrowed particle (A) then overcomes the pinning force in (B).

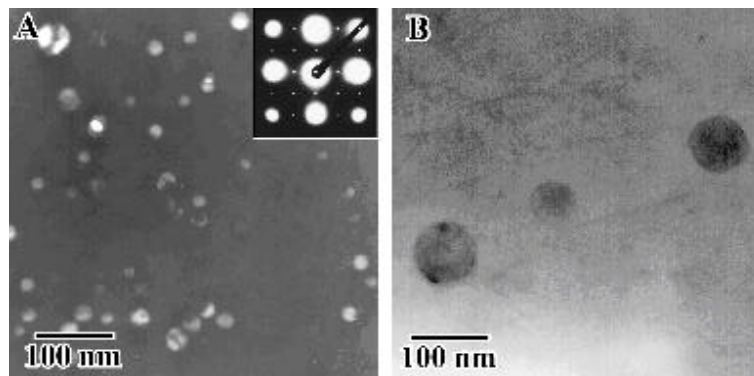


Figure 2. TEM images of Al_3Sc particles following a (a) $300^\circ\text{C}/50$ hr heat treatment and (b) hr heat treatment. The dark-field image in (a) is taken using one of the superlattice spots shown in the inset diffraction pattern and reveals that the precipitates (bright) are very small and coherent with the matrix. The precipitates in (b) are larger, fewer in number and incoherent.

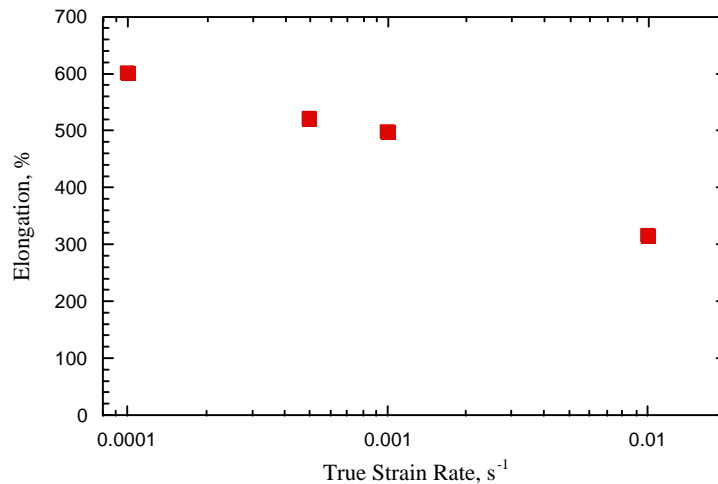


Figure 3. Elongation as a function of strain rate for an Al-4% Mg-1% Mn-0.5% Sc alloy heat treated for 2 hrs. @ 500°C (deformation temperature is 550°C).

Coatings for Reduced Friction and Wear in Micro-electromechanical Systems

D. M. Follstaedt, J. A. Knapp, M. T. Dugger, and T. Christenson, *Sandia National Laboratory*
J. W. Ager III, O. R. Monteiro, and I. G. Brown, *Lawrence Berkeley National Laboratory*

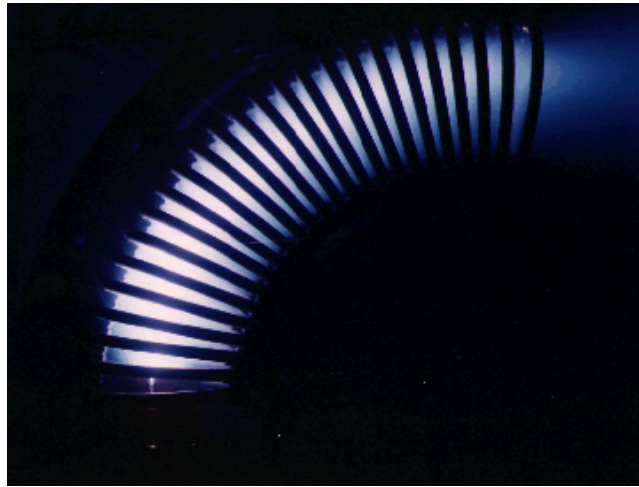
Motivation—One class of micro-electromechanical systems (MEMS) consists of ultrasmall motors and actuators with correspondingly tiny moving parts. The tribological performance (i.e. friction and wear) of these parts is critical to developing reliable MEMS devices. There are unique materials challenges in designing and developing the tribological interfaces in these devices. The parts are usually defined by photolithography, and have very smooth surfaces, which can lead to “stiction,” an effect which stems from the tendency of flat surfaces to stick together. Although loads are low in MEMS due to the small size of the parts, contact dimensions are small leading to high contact pressures, and rotational speeds can be quite high (e.g. 80,000 rpm in recent Sandia prototypes). In addition, the generation of wear debris is of particular concern in MEMS systems due to their small mechanical tolerances. In this Center for Excellence project we are concentrating on a subclass of MEMS devices manufactured by the LIGA process. In LIGA, X-ray lithography is used to generate a high-aspect-ratio “hole” in a photoresist material. Ni metal is electroplated into the molds to form micron-sized parts, which are assembled into the final machine either by hand or by a robot.

Accomplishment—A series of Ni substrates were coated at LBNL with ultrahard, low-stress diamond-like carbon films via a pulsed vacuum-arc plasma process. Previous work in the Center had developed methods to improve the

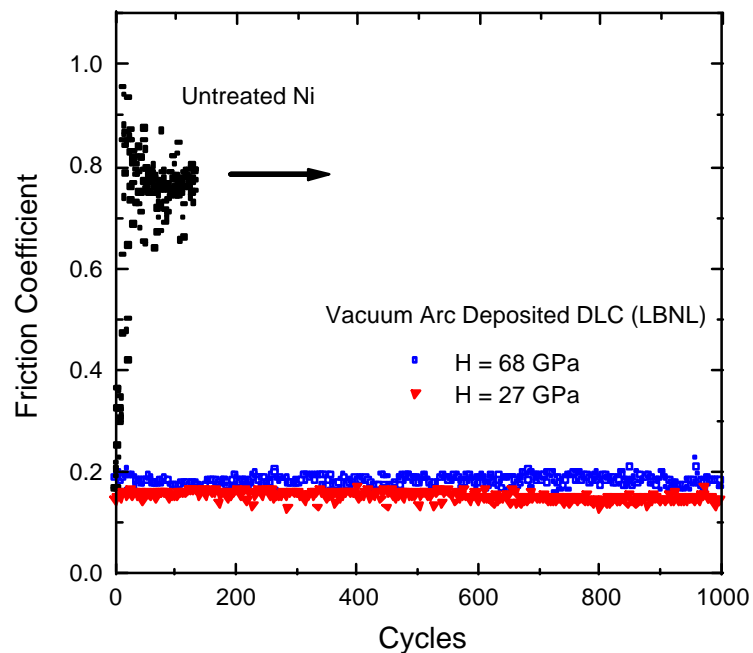
adhesion of these coatings while retaining their high hardness. The coating thickness and hardness were chosen based on the intended wear environment of prototype Sandia applications involving LIGA-manufactured Ni parts. The LBNL plasma deposition process is advantageous over other DLC deposition methods for this application because the deposition may be performed at room temperature, complicated shapes with reasonable aspect ratios may be coated, and if required, extremely hard coatings can be deposited. Moreover, the ability to adjust ion energy with substrate bias leads to improved adhesion of the coating. Tribological measurements performed at Sandia under representative MEMS operating conditions showed that the DLC coating led to dramatic improvements in friction and wear compared to uncoated parts (see figure). Somewhat better friction performance was found for the “softer” ($H = 27$ GPa) film compared to an ultrahard (68 GPa) film.

Significance—Joint work between Sandia and LBNL within this Center of Excellence project has led to the development of a promising wear coating for MEMS actuators and motors. The excellent friction and wear properties of the coating are expected to lead to increased lifetime and reliability of these devices. In future work, the team will address the challenge of coating electroformed Ni parts with high-aspect-ratio geometries such as micron-sized axles and gear teeth.

Contact: Joel W. Ager III, Lawrence Berkeley National Laboratory
Phone: (510) 486 6715 Fax (510) 486 4114 E-mail: ager@lbl.gov



The 90° particle filter with plasma flowing through it as used in the pulsed vacuum-arc deposition of diamond-like carbon films at LBNL.



Friction measurements of Ni substrates in a simulated MEMS environment (unlubricated sliding contact with steel pin, 500 MPa Hertzian contact stress). The graph shows the high friction coefficient and stick-slip adhesion of uncoated Ni and the low friction (<0.2) of Ni coated with LBNL diamond-like carbon. Results are shown for a maximum hardness film ($H = 68$ GPa; for reference, diamond hardness ~ 100 GPa) and for a softer film (27 GPa). Friction coefficient is slightly lower for the softer film.

Finite-Element Modeling of Nanoindentation for Evaluating Mechanical Properties of Thin Films and Implanted Layers

J. A. Knapp, D. M. Follstaedt, S. M. Myers, and J. C. Barbour, *Sandia National Laboratories*
J. W. Ager III, O. R. Monteiro, and I. G. Brown, *Lawrence Berkeley National Laboratory*

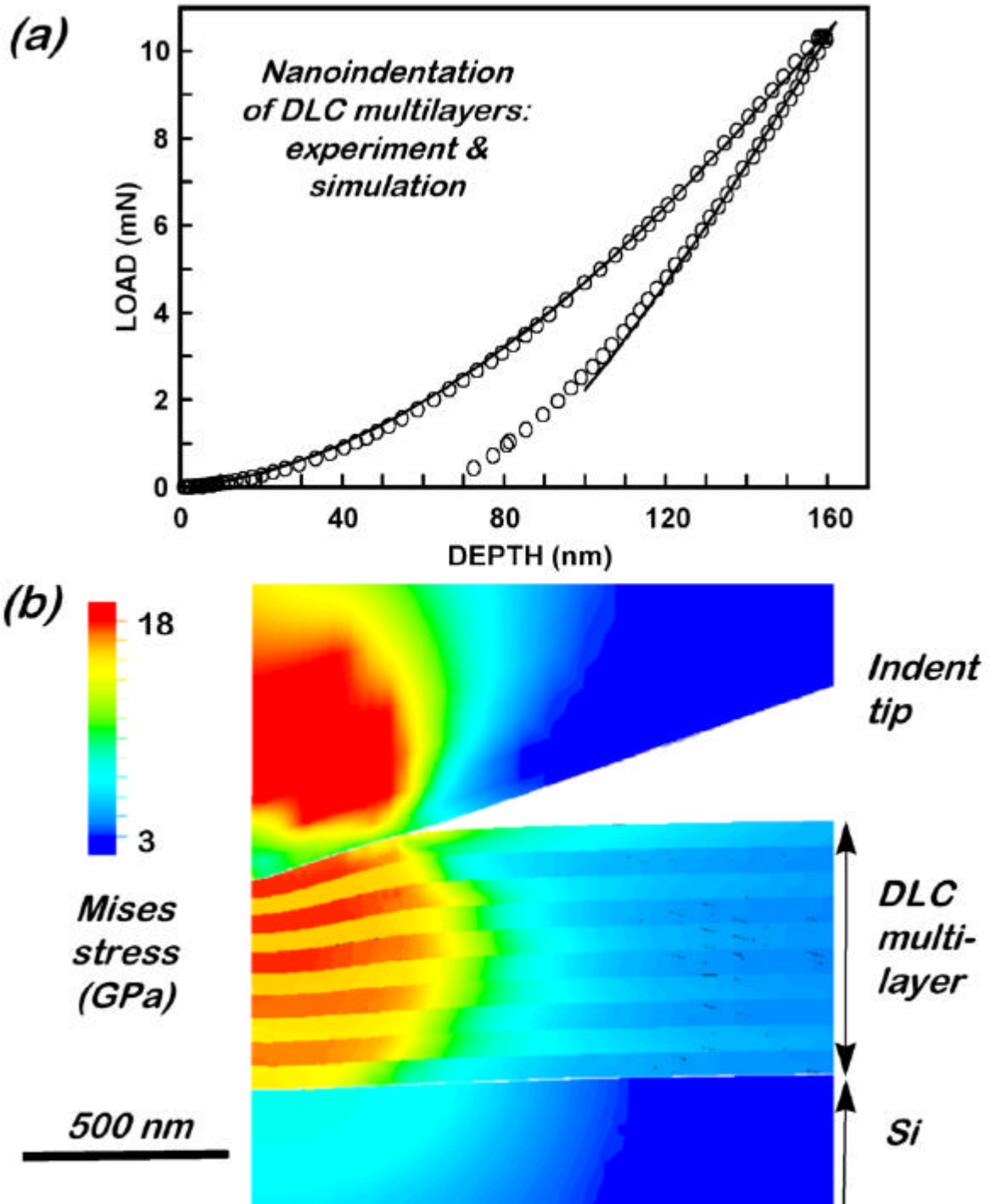
MotivationAs materials applications use smaller structures and thinner coatings, characterization of the mechanical properties of the materials has become more difficult. One method that has become widely accepted is depth-sensing indentation at low loads, or "nanoindentation." However, as the thickness of the materials continues to decrease, obtaining a substrate-independent measure of the mechanical properties of layers becomes increasingly complicated due to the influence of the underlying material. The problems are particularly severe for application of nanoindentation to implantation-modified layers, since the properties of a layer may vary through its depth. For films with hardnesses that may approach that of bulk diamond, the deformation and possible yielding of the indenter tip are additional complications. Since analytical derivation of the mechanical properties is generally not feasible for these cases, we have developed numerical procedures for deducing the intrinsic mechanical properties of thin films and implantation-modified layers, properties independent of the substrate.

AccomplishmentThe methodology we use is based on finite-element modeling of the nanoindentation experiment, using a good fit to the experimental data to infer the mechanical properties of the thin surface structures. The method extracts the yield strength, Young's modulus, and intrinsic layer hardness from indentations as deep as 50% of the layer thickness. We first generate meshes and depth-dependent material property descriptions specific to each sample, and then the simulations of nanoindentation are performed on a

workstation using the commercial, large-strain, finite-element code ABAQUS/Standard. Blunting of the indenter tip, friction between tip and surface, and pre-existing stress in the layers can all be included in the modeling. The two parameters for the layer material which are extracted from the fit of simulation to experiment are the yield strength (defined at a plastic strain of 0.002), and Young's modulus (elasticity). Hardness, a commonly used figure of merit, is then deduced by an additional simulation using the yield strength and elasticity of the layer in a hypothetical bulk "sample". These methods have been applied to a wide range of systems including AlO_x layers formed by O ion implantation, ECR plasma deposition, or pulsed laser deposition, Ti+C implanted Ni and Ni alloys, and "diamond-like" carbon layers (DLC) deposited at LBNL with hardnesses as high as 68 GPa, approaching that of crystalline diamond (~100 GPa). We have recently applied the modeling to nanoindentation of DLC layers deposited at Sandia and of bulk diamond in a collaboration with Nano Instruments, Inc.

Significance-Application of nanoindentation to deposited and ion-implanted thin films has been limited by the lack of convenient tools for modeling the composite, non-linear sample response and extracting the layer properties. Our development of these tools has increased the applicability of nanoindentation testing to very thin layers, composite layers, and modulated structures (see figure). The technique is widely used in our research program and has been transferred to other laboratories in the U.S. and abroad.

Contact: James A. Knapp, Sandia National Laboratories, New Mexico
Phone: (505) 844-2305 Fax: (505) 844-7775 E-mail: jaknapp@sandia.gov



(a) Experimental and calculated nanoindentation force vs. Depth curves obtained from a 10 layer multilayer with alternating hard and soft DLC layers, on Si. The sample was made using vacuum arc deposition at Lawrence Berkeley National Laboratory. (b) Calculated Mises stress in the sample and indenter pin at 160 nm indentation depth, with the scale shown at the left. A 2-dimensional axisymmetric mesh was used for the simulation.

Improved Process for Depositing Thick, Adherent Films of Cubic Boron Nitride

P. B. Mirkarimi, D. L. Medlin, and K. F. McCarty, *Sandia National Laboratories, CA*
J. A. Knapp, *Sandia National Laboratories, NM*

Motivation—Diamond and cubic boron nitride (cBN) are the two hardest known materials, making them natural candidates for hard, protective coatings. In several ways, cBN is superior to diamond. For example, unlike diamond, cBN does not dissolve into iron-containing alloys and has a high resistance to oxidation (at temperatures as high as 1300°C). Recently cBN films have been grown using ion-assisted deposition processes. Unfortunately, the films contain significant levels of residual compressive stress. Because of this, the films do not adhere well to the substrate. Furthermore, film thickness has been limited to about 0.1 micron since thicker films delaminate immediately.

cBN does not readily form in film growth; instead, graphitic BN forms in any process that is not ion-assisted and optimized. It is generally believed that compressive stress may be necessary to form cBN rather than graphitic BN. Clearly, however, to grow thick, adherent films of cBN, it is necessary to reduce the film stress.

Accomplishment—To reduce film stress, but still grow cBN, we made two important changes to the film-deposition process. First, we grew at high substrate temperatures, about 1000°C, rather than the 400-500°C temperatures typically used. Such high-temperature growth dynamically anneals the stress-generating defects. Second, we bombarded the growing film with low-energy ions of about 100 eV, rather than the 400-700-eV ions typically used.

The low-energy ions produce less stress than the high energy ions. Using the new high-temperature, low-ion-energy process, we achieved thick, adherent films of cBN. Figure 1 shows a BN film as analyzed by cross-sectional transmission electron microscopy. The thick films were found to have columnar grains and the crystallinity was significantly improved over that of films grown by previous processes. Using nanoindentation on the thick films, we performed the first accurate mechanical-property measurements of cBN films (see Fig. 2). The films had hardnesses (>60 GPa) matching or exceeding that of bulk cBN. In contrast, films grown by our previous process were significantly softer than bulk cBN.

Significance Our new process shows that cBN films can be grown to the thicknesses required for applications such as protective coatings. Encouragingly, these films are "ultrahard," and only diamond films will be harder. Using the new process, it should be possible to grow films of arbitrary thickness. While still too defective for active electronic applications, the improved crystallinity we achieved is a significant step toward such applications. Finally, our results have implications for the mechanism of cBN growth, an actively debated topic. Grain growth clearly occurs in our process. Since grain growth is not compatible with several of the proposed mechanisms, our results indicate that these proposals can be rejected.

Contact: Kevin McCarty, Sandia National Laboratories, California
Phone: (510) 294-2067 Fax: (510) 294-3231 E-mail: mccarty@sandia.gov

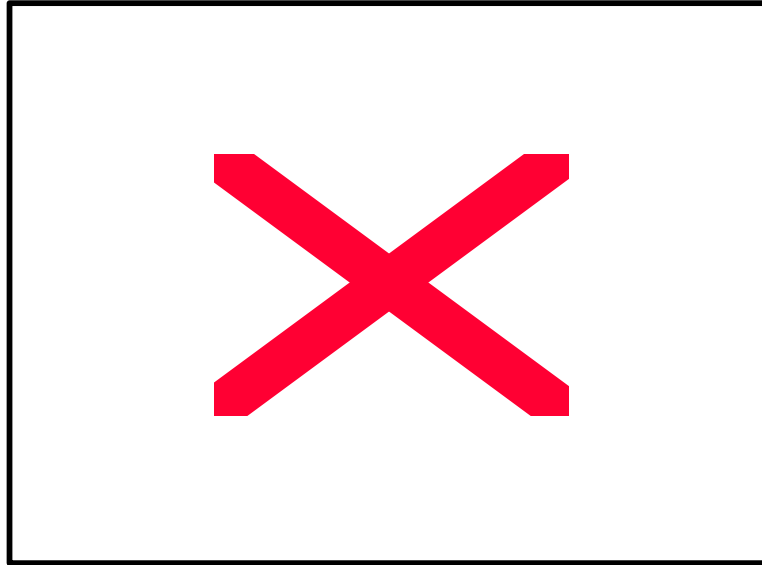


Figure 1. Transmission electron micrograph of a thick cBN film in cross section. This dark-field image was formed using a portion of the (111) diffraction ring of cBN. Thus, the bright regions are columnar grains of cBN, showing that significant grain growth occurs using the deposition process.

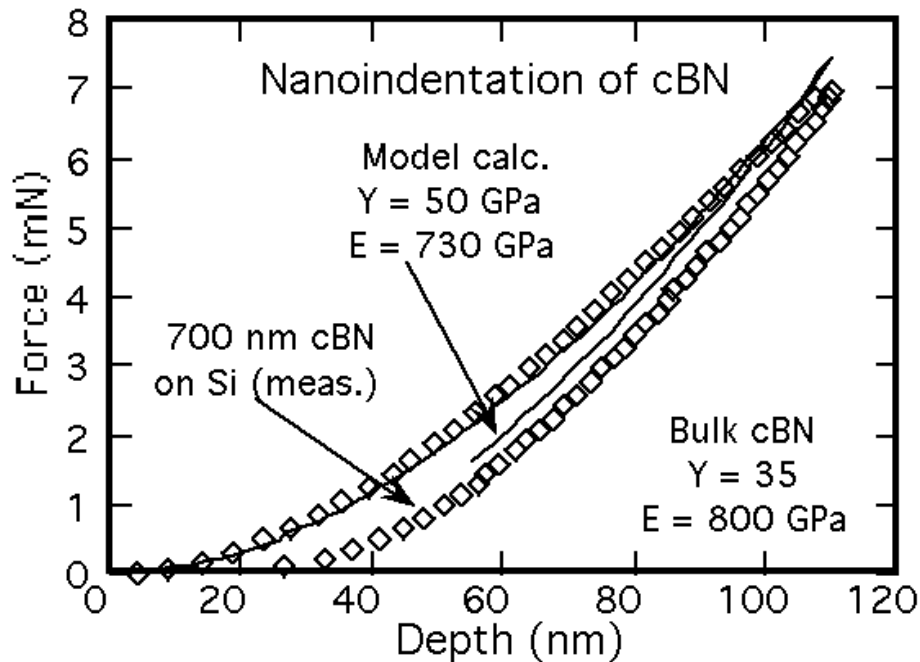


Figure 2. Nanoindentation analysis of a 7000-Å-thick cBN film on a silicon substrate. The symbols represent the experimental data while the solid lines are fits to a finite-element model of the indentation. The left-most trace is the loading curve while the right-most trace is the unloading curve. Analysis of the experimental unloading curve gives a hardness of 60+ GPa, consistent with the results of the finite-element analysis.

Molecular Engineering of Structured Polymer-Polymer Nanocomposites

Douglas L. Gin, Jeff Reimer, *Lawrence Berkeley National Laboratory*
Eric S. Pederson, *Idaho National Engineering and Environmental Laboratory*
Jun Liu, *Pacific Northwest National Laboratory*

Motivation Composite materials properties are highly dependent upon the localized micro- and nanostructures introduced during processing. Control of pore size, anisotropy, distribution, and density induced by means of solution templating techniques offers the possibility for a high degree of structural sophistication in the material. An ordered nanostructure markedly influences attendant materials properties including mass transport, catalytic behavior, and mechanical robustness. Therefore, new processing routes to achieve a specific architecture in the resident matrix are critically needed in order that the material exhibit the desired response. The processing parameters which influence the self-assembly process control the evolving architecture of the material. A fundamental understanding of this relationship is required for the design and synthesis of advanced materials with tailored microstructures.

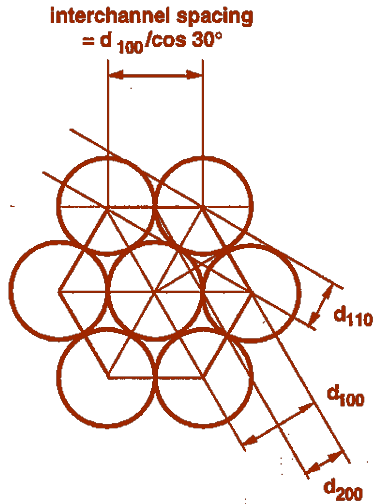
Accomplishment Polymeric materials containing three-dimensional ordered pore nanostructures have been derived from selected monomer precursors having self-assembly properties. Recent activities have shown that a liquid crystal monomer in solution with a water

soluble precursor to PPV (poly-phenyl vinylidene) readily forms the inverse hexagonal phase. Upon photopolymerization, a cross-linked matrix is generated in which the hydrophilic channels subsequently fill with the PPV precursor. Heating causes polymerization of the PPV-precursor to PPV within the channels. XRD measurements are used to characterize this structure and also to show that the structure is maintained upon heating and subsequent matrix polymerization as shown in the accompanying Figure.

Significance Materials having controlled nanoarchitectures often exhibit very desirable, but often unexpected, properties. Pore ordering in ceramic phases results in effective ion exchange or separation membranes which can be used at high temperatures. Applications of these materials to gas separation or waste water clean-up are currently under investigation and likely will provide for increased separation efficiency and associated cost savings. The display and photonics industries also could benefit from nano-ordered fluorescent polymers which recently have been shown to exhibit enhanced emission due to the ordering.

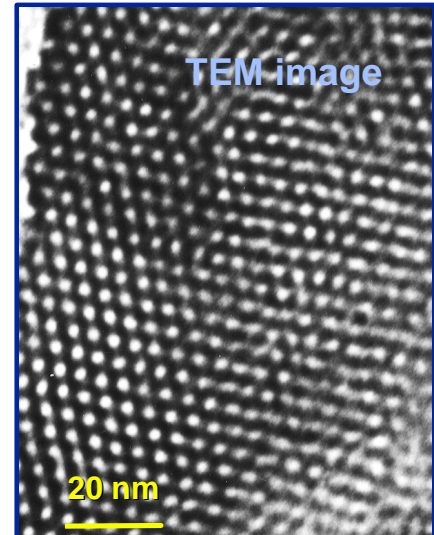
Contact: Douglas Gin, Lawrence Berkeley National Laboratory
Phone: (510) 642-7756 Fax: (510) 643-6232 E-mail:
gin@chemgate.cchem.berkeley.edu

Liquid Crystal Monomer + Organic Photoinitiator + PPV Precursor Polymer

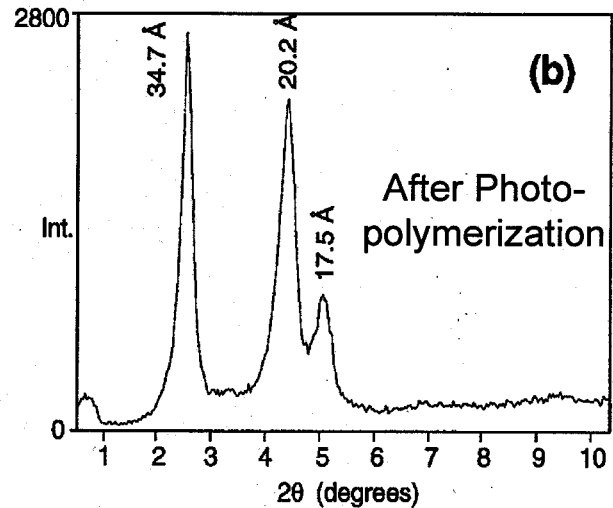
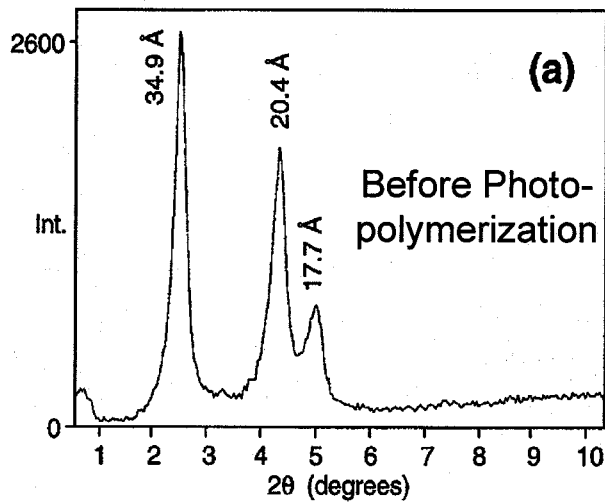


$h\nu$

heat



PPV Ordered Composite



Synthesis of an ordered polymer poly-phenyl vinylidene (PPV) nanocomposite requires combining a liquid crystal (LC) monomer with an organic photoinitiator in water containing a soluble precursor to the PPV polymer. The LC self organizes into a hexagonal arrangement (upper left) which is characterized by means of low angle X-ray diffraction. Little change is seen in the scattering pattern (bottom) upon photopolymerization. The ordered void microstructure accommodates the PPV precursor which undergoes thermal polymerization within the filled interstices of the composite. An image of the representative nanostructure so-derived is shown in the TEM micrograph.

Conformation and Dynamics of Structure-Directing Molecules in Tailored Composites

Jun Liu, Li-Qiong Wang, and Bill Samuels, *Pacific Northwest National Laboratory*
Eric S. Pederson, *Idaho National Engineering and Environmental Laboratory*

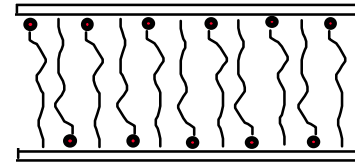
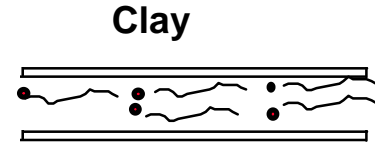
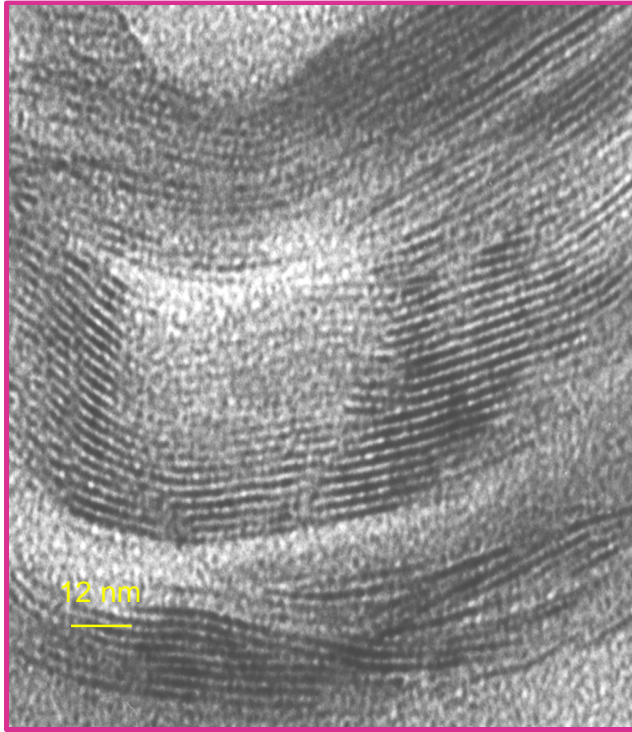
Motivation Manufacturing needs require development of light weight polymer composites which are based upon percolation of a polymer phase through a layered alumino-silicate ceramic. If the clay is uniformly dispersed, it acts not only as a crosslink to mechanically strengthen the composite but functions to improve the thermal stability of the polymer. However, reproducible processing routes to achieve homogeneous dispersion of the layered ceramic material in the polymer and drive entrainment of the polymer chains within the layers continue to be elusive. One approach involves selection of an appropriate surfactant to mediate both processes. The mechanism by which the surfactant influences dispersion phenomena is relatively well understood, but its ability to influence the layer spacing in clays requires further study.

Accomplishment ^{13}C NMR measurements of surfactant-clay mixtures in aqueous solution provide the ability to probe the surfactant molecular conformation at the clay interface. Recent results indicate that the chemical nature and size of the surfactant binding group influence the surface occupancy of the adsorbed surfactant. A critical occupancy is required for expanding the clay layer. The NMR measurements have identified two distinct

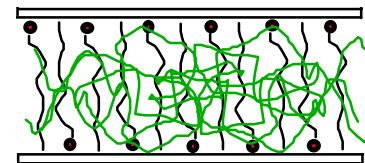
possible conformations (all-trans and gauche) of a subject surfactant (octadecylamine) in clays regardless of the d-spacing resident in the clay layers. The resident conformation is likely related to the wetting properties of treated clays used in ceramic-polymer composites. The surfactants, in either conformation, show restricted mobility within the clay galleries. While the all-trans conformation has not been observed for surfactants adsorbed to silica particles or onto mesoporous silica structures, it is present in these layered materials. The NMR results have been correlated with distinct TEM-determined nanostructures.

Significance Magnetic resonance measurements can be used to probe surfactant ordering phenomena in complex mixtures. The final architecture derived from a selected set of processing conditions can be inferred from these measurements prior to isolation of the material. As a direct result, NMR spectroscopy can be used to derive nanoarchitecture phase diagrams. Based upon the NMR measurements, selection of an appropriate surfactant which would act to increase the layer spacing to a specified separation, becomes relatively straightforward. Subsequent entrainment of the polymer phase within the lamellar layers can then proceed readily to form the molecular composite.

Contact: Jun Liu, Pacific Northwest National Laboratory
Phone: (509) 375-2616 Fax: (509) 375-2186 E-mail: j_liu@pnl.gov

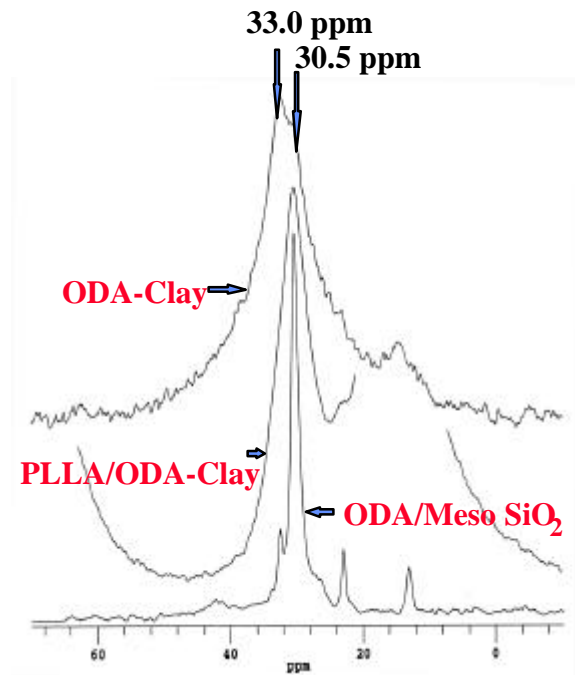


PLLA/Clay



The all-trans conformation of ODA in clays disappears when the polymer (PLLA) is inserted into clays.

^{13}C NMR measurements are used to probe surfactant conformation within the galleries of layered clay-like aluminosilicates. Certain chain conformations induce layer spreading provided that a critical interlayer surface density of surfactant molecules has been achieved. The adsorption cross-section is controlled by the size and charge density of the surfactant head group. Once layer separation has been achieved, entrapment of a polymer, PLLA, becomes possible allowing formation of a true molecular composite.



Modeling Properties of Polymer Blends

A. Habenschuss, *Oak Ridge National Laboratory*

J. G. Curro, *Sandia National Laboratory, New Mexico*

J. McCoy, C. Stevenson, *New Mexico Institute of Mining and Technology*

Motivation—A refined theoretical approach is required for understanding polymer melt behavior and the miscibility and phase stability of polymer blends. One approach, based upon a statistical mechanical theory of polymer liquids and blends, is termed the off-lattice Polymer Reference Interaction Site Model (PRISM). It is a microscopic integral equation theory which includes the important effects of non-random mixing and intrachain molecular architecture, leading to a molecular-level prediction of polymer alloy structure and miscibility. PRISM can systematically investigate the influence of local chemical architecture, global structure, intermolecular forces, and the thermodynamic state on the blend properties. The novelty of this approach is to provide a foundation for understanding the factors controlling miscibility in polymer mixtures.

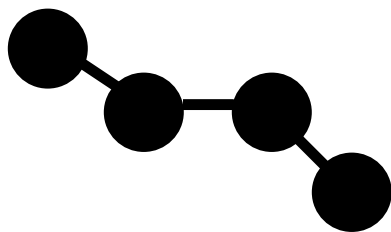
A fundamental input to the PRISM theory, which is used to calculate polymer blend structure and thermodynamics, is the single chain structure (i.e. the intramolecular structure) of the blends' components. PRISM then determines the molecular packing geometry (the intermolecular structure) based on the single chain structure and intermolecular atom-atom potentials. The single chain structure (bond lengths, bond angles, torsional potentials) can be derived from small molecule analogues of polymers, such as the alkanes for polyethylene. The objective of this program is to obtain intramolecular structure information from x-ray

scattering on small molecule analogues that can subsequently be used as input to PRISM theory to predict the properties of saturated hydrocarbon polymers (eg. polyolefins).

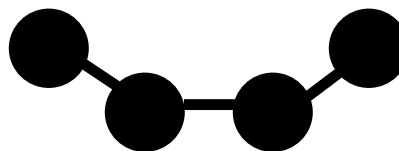
Accomplishment—The intramolecular parameters for a series of linear alkanes (bond lengths, bond angles, and torsion angles) were extracted from the structure function obtained from wide-angle X-ray scattering (WAXS). These were then used to guide the calculation of the single-chain structure functions of some polyolefins. Finally, PRISM was used to calculate the intermolecular structure function. A comparison of the experimental structure functions with the PRISM results is shown in the Figure. Excellent agreement is seen between the experimentally measured and computationally derived structure. This approach to polymer structure is currently being extended to halogenated hydrocarbons.

Significance—Polyolefins and their halogenated derivatives constitute the largest segment of the polymer market. It is economically more desirable to "engineer" polymer blends from existing materials to achieve some targeted property rather than developing new polymers with the required properties. PRISM can systematically examine the influence of the properties of homopolymers on blend structure, miscibility, and thermodynamics. The results of this work will provide a foundation for future progress in the design of advanced polymer blends having targeted properties.

Contact: T. Habenschuss, Oak Ridge National Laboratory
Phone: (423) 574-6018 Fax: (423) 576-5235 E-mail: tth@ornl.gov



Trans

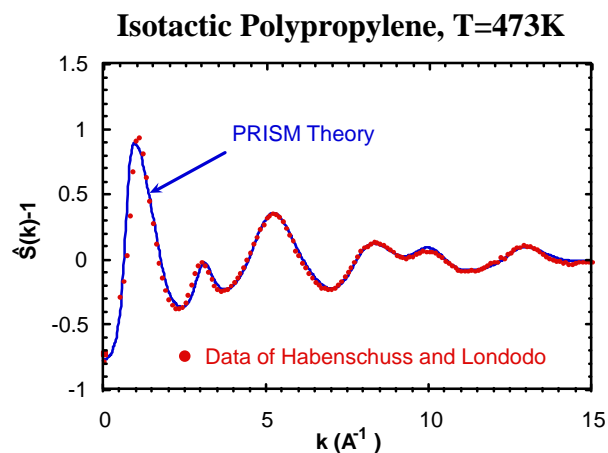
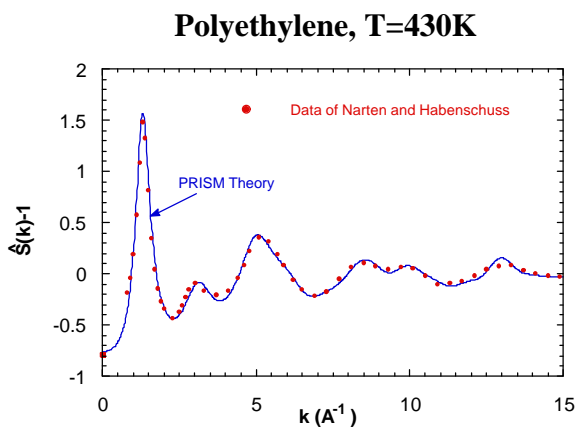


Gauche

Parameters

Bond Length: C-C Bond Angle: C-C-C

Torsion Angle: C-C-C-C



Intramolecular parameters (bond length, bond angle, and torsion angle) are determined from the structure function of liquid alkanes containing 1 to 20 carbon atoms. Based upon these values, the intermolecular structure of extended alkane-like polymers (polyethylene or isotactic polypropylene) have been calculated using PRISM. Excellent agreement between the calculated structure functions and those determined from WAXS data is evident in the figure.

A Novel Approach to Understanding Weld Pool Solidification Using Metal-Analogue Systems

R. K. Trivedi and M. A. Eshelman, *Ames Laboratory*
S. A. David and J. M. Vitek, *Oak Ridge National Laboratory*

Motivation Although significant progress is being made in advancing the science of welding, great challenges still exist in our scientific understanding of microstructure and defect formation that is crucial to the reliability of welds. This is because the dynamics of microstructure evolution and defect formation are quite complex, and they cannot be examined in opaque metallic systems in which the precise physics that govern the microstructure and defect formation is inferred only from the welding that is completed. To circumvent this barrier, we have developed a welding analogue by using a transparent system. This has allowed us to quantitatively study for the first time the complex dynamics of grain selection, weld pool shape, defect nucleation and growth, and melting as functions of composition, power input and welding rate.

Accomplishment The model systems of pure succinonitrile and succinonitrile-acetone were used for the initial study. This is because succinonitrile has a cubic crystal structure, small entropy of fusion and small anisotropy in interface properties, properties that are also exhibited by metallic systems. Thus, these systems allow one to quantitatively analyze the dynamics of microstructure and defect formation which will be identical to those in metallic systems. These dynamical changes were recorded on a video and then quantitatively

analyzed by using image analysis. Linear welds in pure succinonitrile were carried out to show the quantitative changes in the shape of the weld pool as a function of welding speed. The pool shape changed from nearly circular to elliptical to tear-drop shape as the welding speed was increased (see figure). The results were compared with the existing model to establish the validity of the use of the model system to simulate metallic welding. Linear welds in the succinonitrile-1.2% acetone revealed several new features which showed significant differences in weld pool shape, dendritic branching modes, defect formation, epitaxial growth and grain growth processes as the welding speed was increased. The fundamental aspects of these changes are being analyzed quantitatively. A preliminary video has been put together to show the potential of the technique.

Significance The ability to observe and quantitatively analyze the complex dynamics of weld pool solidification and defect formation has an enormous potential for understanding the fundamental scientific issues in welding and for using this understanding to develop welds with better quality and integrity. Some of the crucial issues in welding, such as origin of porosity and hot cracking, can be examined in situ for the first time, which will allow one to develop precise models for reliable welding.

Contact: R. K. Trivedi, Ames Laboratory
Phone: (515) 294-5869 Fax: (515) 294-4291 E-mail: trivedi@ameslab.gov

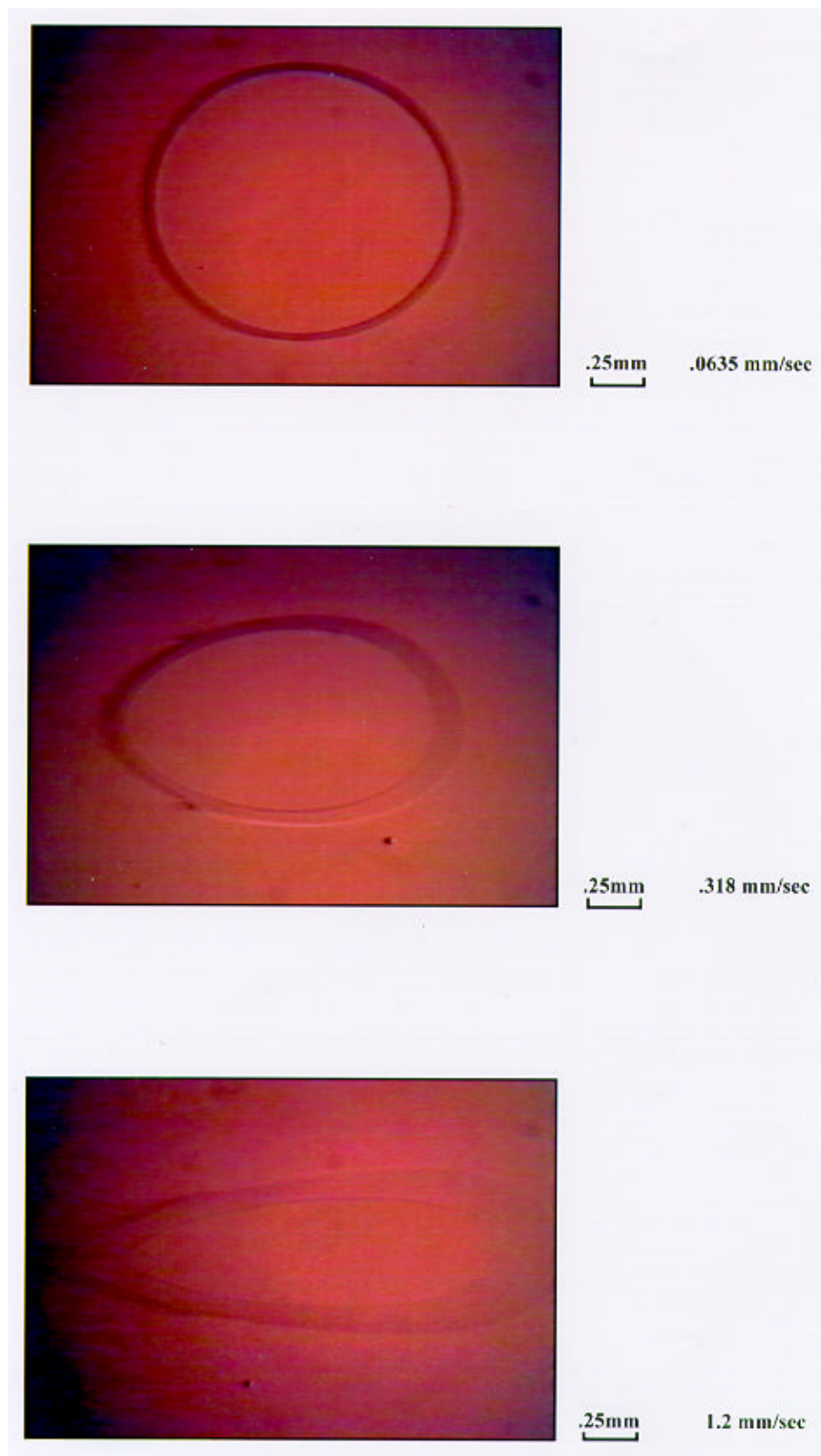


Figure shows the effect of welding speed on the weld pool shape. Weld melt runs were made on succinonitrile.

*Joining of SiC-Based Ceramics for Elevated Temperature Applications**

B. H. Rabin, *Idaho National Engineering & Environmental Laboratory*

P. A. Craig, *DuPont Lanxide Composites, Inc.*

T. V. Narayanan, *Foster Wheeler Development Corporation*

Motivation SiC-based ceramics and composites offer the potential for significant efficiency improvements in power generation and energy conversion systems. Practical and reliable ceramic-to-ceramic and ceramic-to-metal joining techniques are required to fully realize the advantages of these materials in industrial applications. Numerical modeling capabilities are also needed to support joining technique development and to assist in joint behavior prediction and evaluation. Successful joining methods will permit the fabrication of large and complex shaped parts, and will allow integration of ceramic components into existing structures. The goal of this project is to develop joining techniques applicable to SiC ceramics and fiber-reinforced SiC matrix composites, with emphasis on producing ceramic-to-ceramic joints for use in elevated temperature structural applications.

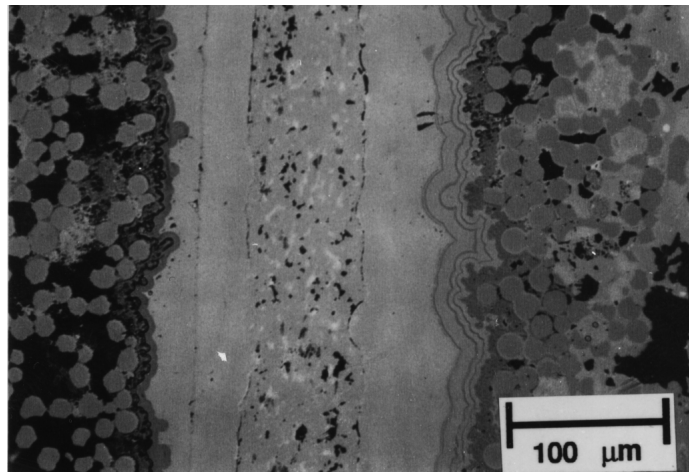
Accomplishment Research conducted at INEEL has led to the development of a technique which permits the fabrication of SiC-to-SiC joints suitable for elevated temperature applications. In this process, which employs methods similar to those used to manufacture commercial reaction bonded silicon carbide, liquid silicon capillary infiltration of SiC+C tape cast precursors is carried out at ~1450°C. Joints having room temperature strengths exceeding 250 MPa are obtained, and joint strengths are maintained at temperatures up to ~1200°C. Joining can be accomplished without the need for high pressure equipment, therefore the technique can be modified to allow in-field component fabrication and repair. Recent equipment and process improvements at INEEL have allowed large tubular structures to be fabricated. The figure shows a 3.5-inch OD

pressureless sintered SiC tube that was cut, re-joined, and later tested under high temperature and pressure at ORNL. Also shown is a micrograph of the polished cross section of a joint between two pieces of SiC/SiC continuous-fiber ceramic composite made by DuPont Lanxide's CVI process. The joint material consists primarily of SiC and Si, so there is little property mismatch and therefore low residual stress in the joints. Extensive modeling capabilities have also been developed for predicting residual stresses and thermomechanical behavior of dissimilar material joints and graded materials, an important tool for further development of useful ceramic-to-metal joining methods.

Significance The ability to fabricate SiC-to-SiC joints having excellent elevated temperature properties will allow the industrial utilization of SiC in numerous applications where higher operating temperatures result in improved energy efficiency. For example, collaboration with Foster Wheeler is focused on the development and construction of an industrial scale high pressure SiC heat exchanger using commercially available pressureless sintered SiC. Work with DuPont Lanxide Composites is examining the applicability of the joining method to fiber-reinforced SiC composites which offer the possibility for improved reliability in applications such as gas turbine components, radiant burner tubes, petrochemical processing systems and heat exchangers.

*Supported by the Division of Materials Sciences, Office of Basic Energy Sciences, Office of Industrial Technologies, and Office of Fossil Energy, U. S. Department of Energy.

Contact: Barry Rabin, Idaho National Engineering & Environmental Laboratory
Phone: (208) 526-0058 Fax: (208) 526-0690 E-mail: bhr@inel.gov



Upper Figure - Joined sintered SiC tube used in high temperature and pressure testing for heat exchanger applications Lower Figure - Optical micrograph showing the microstructure of the joint produced between two pieces of SiC/SiC continuous-fiber ceramic composite.

Improved Properties of Joints Between SiC/SiC Composites from Further Development of Low Temperature Bonding Process

O. Unal, I. E. Anderson, S. I. Maghsoodi, M. Nosrati, and T. J. Barton, Ames Laboratory
P. A. Craig, DuPont Lanxide Composites, Inc.
A. Szweda, Dow Corning and W. Bustamante, Amercom

Motivation SiC-based ceramic composites have been receiving much attention for their potential in high-temperature applications such as gas turbines, internal combustion engines, etc., due to their favorable chemical, thermal and mechanical properties. However, since the manufacturing of large and complex ceramic parts cannot be produced economically, it has been of great interest to develop joining methods which would allow the small ceramic pieces to be bonded to assemble useful end products. It is also very desirable that the available joining methods be simple and have wide-range uses, including on-site assembly and repair work in the field (air atmosphere). Moreover, it is important that the joining methods utilize low temperatures during the processing.

In this Center project a number of coordinated, alternative approaches to SiC-SiC joining are being pursued. Our approach is summarized below.

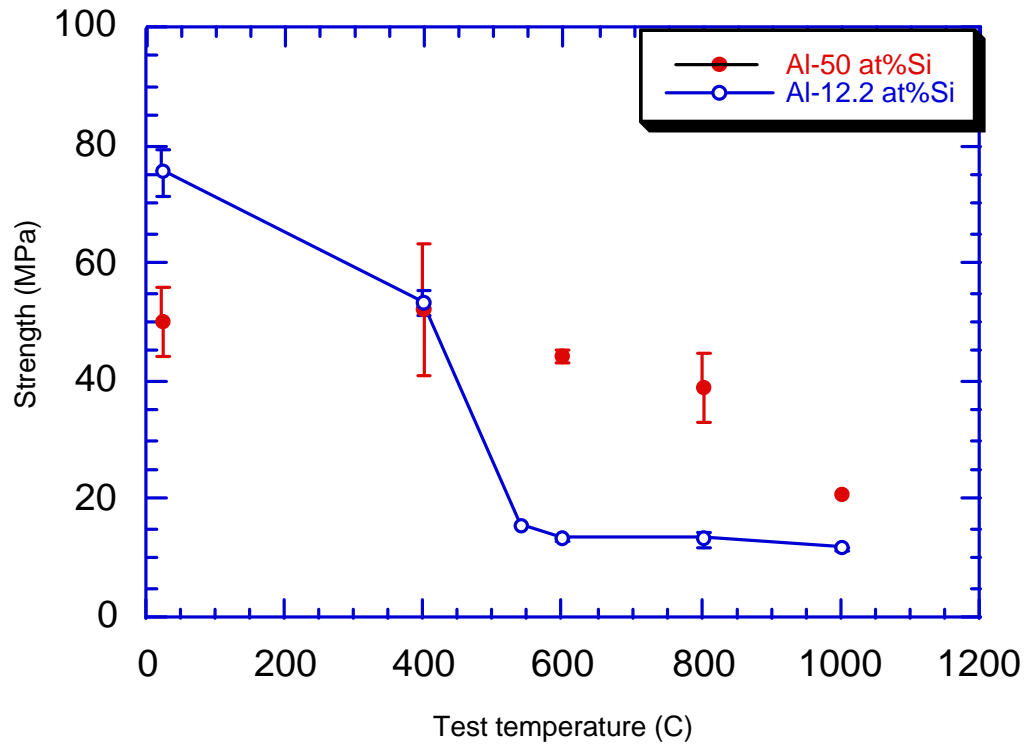
Accomplishment We are developing a relatively low temperature approach to join SiC parts. The bonding agent for the joints uses a preceramic oligomeric polymer, Al-Si alloy powder and boron powder. A unique feature of this low temperature joining approach is that the strength obtained at the joint is due to the Al₂O₃ formation at 1200°C in air. The commercial ceramic composites (SiC/SiC) used in our joining experiments contained Nicalon fibers either in a CVI matrix (provided by Dupont and Amercom) or in a melt infiltrated matrix (provided by Dow Corning). Test specimens were made as butt-joints. The asymmetric four point bend (AFPB) test, which was developed during this study to

test miniature joint specimens, was used to measure shear strength at high temperatures. This method proved to be very valuable since the bond strength and interfacial shear strength values can be measured on the same specimen geometry. Initial tests focused on the joint properties based on a filler material, which contained Al-12.2 at % Si alloy powder. Test results showed remarkably high room temperature strength values for such a low curing temperature. However, due to high Al content in the powder, the joint region contained a large amount of residual Al. As a result, high temperature properties were unsatisfactory. For improvement, Al content of the powder was reduced (Al-50 at % Si). The preliminary tests showed substantial improvement of the high-temperature strength (see figure) which is the desired goal. Work is continuing to optimize this strength by further adjustment of the filler composition, including trials of a Dupont preceramic polymer.

Significance There are several methods currently being used for ceramic joining such as fusion, solid-state, etc. However, the problem associated with these methods is that they often require temperatures which are unacceptable for ceramic composites containing Nicalon fibers. This is because Nicalon fibers, which are used commonly in ceramic composites, dissociate and thus, lose their strength above 1200°C. Therefore, it is important that the curing temperature be maintained below 1200°C. Al₂O₃ is the primary phase forming at low temperatures in our process. The implication of this current approach is that this method is simple, practical and cost effective.

Contact: I. E. Anderson, Ames Laboratory
Phone: (515) 294-4446 Fax: (515) 294-8727 E-mail: andersoni@ameslab.gov

Properties of Joints Between SiC/SiC Composites from Low Temperature Bonding Process



Bond strength of ceramic joints as a function of test temperature. Tests were carried out on the ceramic joints, which were made using a bonding agent containing Al-Si alloy powder of two different compositions. Joint strength of Al-rich powder (Al-12.2 at % Si) decreased sharply at elevated temperature due to the presence of large amount of residual Al. Reducing Al content in the starting powder (Al-50 at % Si) and use of finer sized powder (diam. < 5 μm) improved the high temperature properties significantly through the better transformation of Al to Al_2O_3 .

Nanocrystalline Composite Coercive Magnet Powder

D. J. Branagan, T. A. Hyde, C. H. Sellers,
Idaho National Engineering and Environmental Laboratory
R. W. McCallum, K. W. Dennis, and M. J. Kramer, *Ames Laboratory*

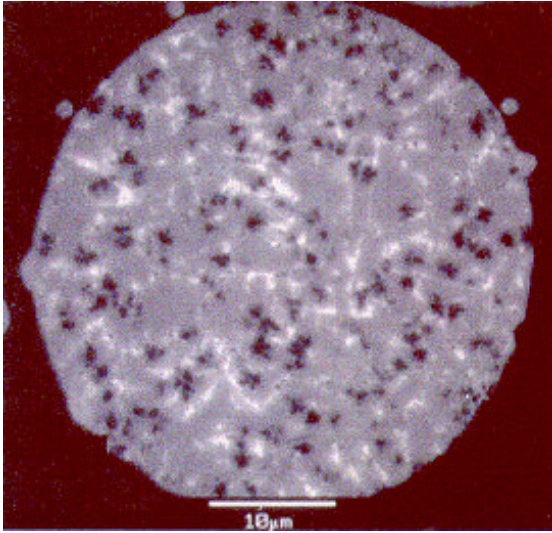
Motivation Improvements in the synthesis and processing methods of hard magnetic materials has broad impact on technologies of interest to the DOE, especially for Energy Efficiency. The impact of more efficient permanent magnet motors is especially high where weight, size, and power density are important. Since many electronic components and sensors utilize permanent magnets, developing cheaper, stronger, and higher service temperature permanent magnet materials would also affect many key consumer and military devices. In addition, developing alternate and cheaper processing methods to produce these high energy permanent magnets would increase use of these materials and allow market penetration in new applications. Specifically, the production of isotropic powder is a vital industrial need, since powder is used in the manufacture of bonded magnets, which can be processed into virtually any shape and with multiple poles. These bonded powder magnets have experienced the most rapid growth of any magnet type.

Accomplishment Atomization techniques for the primary production of coercive magnet powders have never been developed commercially due to technical difficulties related to issues such as broad distribution of particle sizes, phase separation and the formation of metastable phases. In order to design advanced alloys for atomization, we have developed a metallurgical approach toward alloying which led to the fabrication of permanent magnets based on the quinary Nd-Fe-B-Ti-C system. Since titanium and carbon have no equilibrium solid solubility (below detectable limits) in the

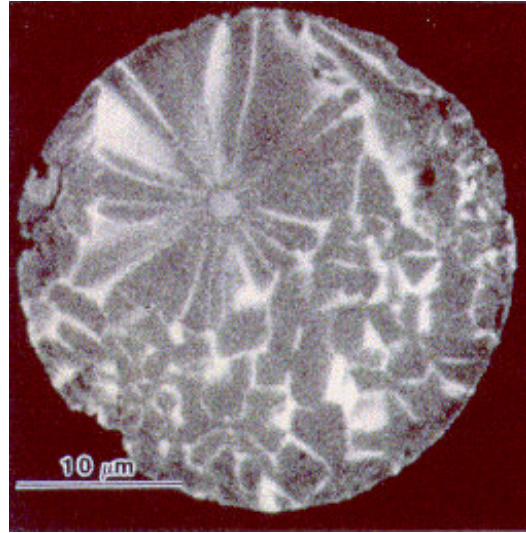
hard magnetic phase, a composite microstructure can be formed consisting of $\text{Nd}_2\text{Fe}_{14}\text{B}$ grains and TiC precipitates at the grain boundaries. An additional bonus of Ti/C additions, is a large increase in the glass forming ability of these alloys which allows metallic glasses to be produced by atomization methods. This is important since by crystallizing from an amorphous precursor, a very fine nanocrystalline (<100 nm) composite microstructure can be formed with grain sizes below the single domain particle diameter resulting in optimum magnetic properties.

Significance Atomization processing of these new alloys resulted in significant improvements in hard magnetic properties and processability over previous alloys, allowing the possibility of near term, high volume, low cost production by atomization methods. The improvements in properties and processing characteristics developed collaboratively at the INEEL and at Ames Laboratory will allow industry to develop better magnets for use in more energy efficient motors for industrial, automotive, and consumer applications. Furthermore, with the successful development of a new process (atomization) and a new product morphology (fine spherical powders), new applications and ways to utilize rare earth permanent magnets will be developed, especially in bonding and injection molding applications. For example, such advances may allow motor manufacturers to simplify and reduce processing cost by injection molding permanent magnets directly into the rotor or stator of a permanent magnet motor instead of assembling the magnets separately.

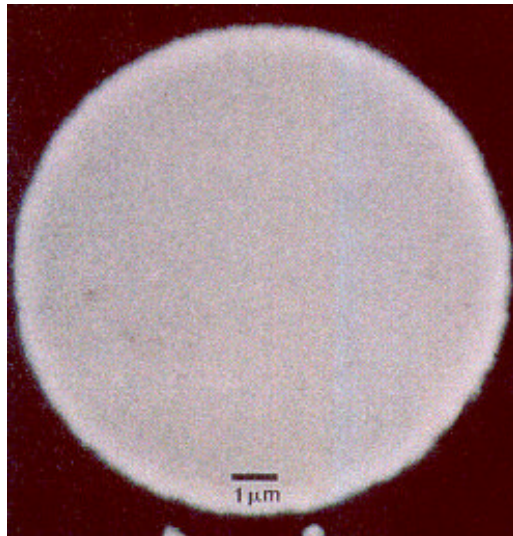
Contact: C. H. Sellers, Idaho National Engineering and Environmental Laboratory
Phone: (208) 526-0119 Fax: (208) 526-2814 E-mail: chs2@inel.gov



1st Generation



2nd Generation



3rd Generation

The microstructures of three generations of gas atomized Nd-Fe-B powders are shown. In the 1st generation, dendritic growth of iron resulted in very low coercivities. In the 2nd generation, a rare earth rich eutectic phase, results in low remanence. In the 3rd generation, near optimum nanoscale microstructures are achieved resulting in good magnetic properties.

Epitaxial Exchange-Spring Magnets

J. S. Jiang, E. E. Fullerton, C. H. Sowers, J. E. Pearson, and S. D. Bader,
Argonne National Laboratory

Motivation High-performance permanent magnets provide opportunities for increased efficiency in energy production and energy systems. The recently proposed ‘exchange spring magnets,’ which are composed of exchange coupled hard- and soft-magnetic phases, have the additional advantage of reduced rare-earth content and improved mechanical properties and corrosion resistance. Recently, nano-crystalline composite magnets have been produced by bulk processing methods such as melt-spinning and mechanical alloying. However, the random nature of these materials prevents them from achieving the full potential of exchange hardening, and makes optimizing the hard-magnet properties largely a ‘trial-and-error’ process.

Accomplishment A model materials system has been designed where virtually all aspects of the exchange spring-coupling phenomenon can be systematically controlled. This has allowed for direct comparison with a theoretical model and provides a more realistic prediction of achievable energy product in exchange-spring magnets.

Using a buffered epitaxial growth method, *a*-axis and *b*-axis oriented SmCo alloy films have been synthesized by sputter deposition onto single-crystal MgO substrates with different orientations. The *a*-axis oriented films have a twinned bicrystal structure which results in an in-plane four-fold magnetic anisotropy and coercivity that is thickness-independent, while the *b*-axis oriented films have in-plane uniaxial anisotropy with room-temperature coercivity as large as 3.4 T and a 20-T anisotropy field which is consistent with bulk intrinsic values (See Figure 1).

The epitaxial hard SmCo layers were incorporated into bilayer and superlattice structures with Fe and Co as the soft layers. The demagnetization of the soft layers is fully reversible as expected for an exchange-spring magnet. The maximum energy product $(BH)_{\max}$ is increased from ~11 MGOe for a single SmCo film to ~14 MGOe for a superlattice composed of 100-Å Co and 450-Å SmCo layers. A micromagnetic model which utilizes anisotropy and exchange constants characteristic of the individual layers was developed to describe the magnetization reversal process and to provide detailed information on the energetics of magnetic domain-walls in the hard and soft layers. Model calculations for a series of bilayer structures illustrate the dependence of $(BH)_{\max}$ on the layer thicknesses and indicated that very large values of energy product are attainable in exchange-spring structures where the hard and soft layers are on the nanometer scale (see Figure 2).

Significance Although bulk materials are needed for many permanent-magnet applications, thin-film magnetic structures are naturally useful for a variety of magneto-electronic devices. This well-characterized model system developed in the current work permits the testing of modern micromagnetic theories, and the investigation of the magnetic properties can serve as a guideline for the development of more complex nanostructures and the for the optimization of the hard-magnet properties in bulk magnets.

The present work is being complemented by high resolution TEM and optical imaging studies at LBNL of the chemical and magnetic microstructure aimed at understanding the high coercivity of the films (see following brief).

Contact: S. D. Bader, Argonne National Laboratory
Phone: (630) 252-4960 Fax: (630) 252-9595 E-mail: bader@anl.gov

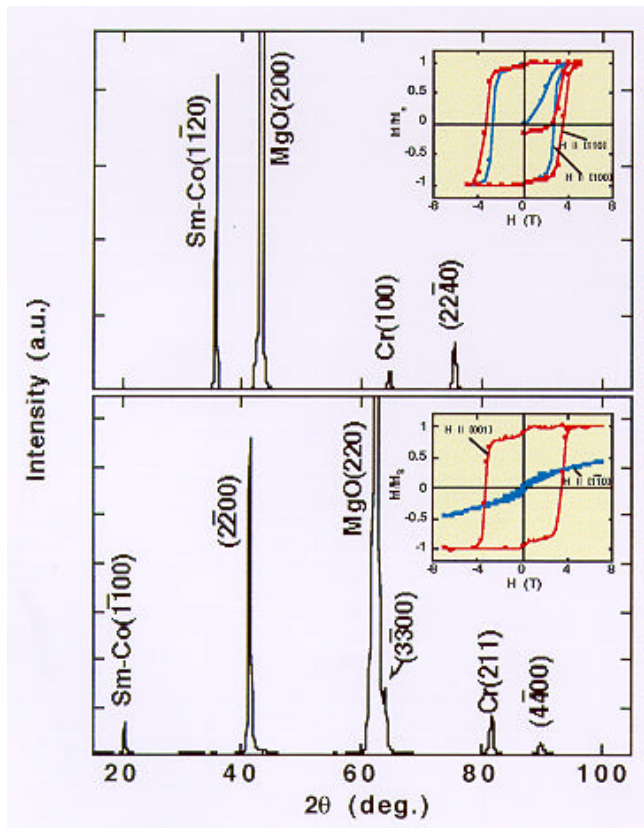
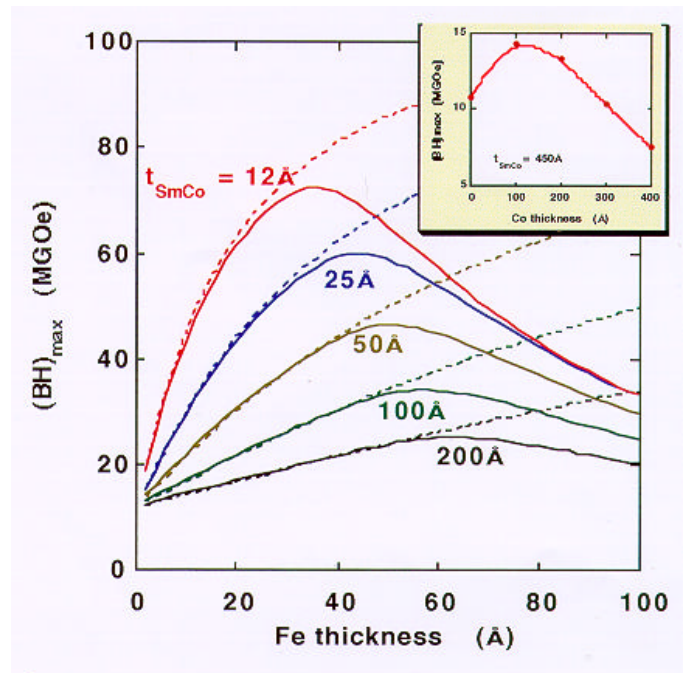


Figure 1. XRD results for epitaxial Sm-Co films grown *a*-axis oriented (top panel), and *b*-axis oriented (bottom panel) simultaneously onto Cr-buffered single-crystal MgO substrates. The insets are room-temperature hysteresis loops with the magnetic field applied along different in-plane directions showing the four-fold and uniaxial magnetic anisotropy.

Figure 2. Calculated $(BH)_{\max}$ for SmCo/Fe bilayer structures with different layer thicknesses. The dashed curves are $(2\pi M_s)^2$, the ultimate theoretical limit for $(BH)_{\max}$. Inset: Experimentally measured $(BH)_{\max}$ for *a*-axis oriented [SmCo/Co] superlattices.



*Magnetic Anisotropy and its Microstructural Origins:
Advances in Electron-Optical Characterization*

Kannan M. Krishnan, M. Benaissa, K. Verbist and C. Nelson,
Lawrence Berkeley National Laboratory

Motivation—Much of the recent enhancement in hard magnet performance has been achieved by developing materials with larger magnetocrystalline anisotropy. However, it is well known that even the best commercial hard magnets only achieve about 50% of the theoretical maximum energy product. In practical alloys, microstructural features such as grain size and shape, phase distribution, grain boundary type, orientation between grains and defects play key roles. Moreover, domain wall pinning at defects within grains or nucleation of reverse domains at grain boundaries or other secondary phases are critical microstructural mechanisms that determine the coercivity of these materials. Since the domain wall widths are inversely proportional to the magnetocrystalline anisotropy, rare-earth based permanent magnets have typical domain wall widths of 10 nm. In order to understand coercivity mechanisms the physical, chemical and magnetic microstructure of these materials must be investigated at the highest level of resolution using the best electron optical imaging techniques available. We present results from our electron microscopy investigations of epitaxially grown Sm-Co thin films where atomic scale defects due to local compositional variations (polytypoids), observed only in high resolution electron microscopy, could explain their large coercivities. We also discuss a novel differential phase contrast imaging technique capable of quantitatively mapping domains at 50 nm resolution.

Accomplishment & Significance—Sm-Co thin films synthesized at ANL with very high in-plane anisotropies have been extensively

studied by transmission electron microscopy in conjunction with magnetic measurements. Two substrate orientations, MgO(100)/Cr(100)/SmCo(1120) and MgO(110)/Cr(211)/SmCo(1100) were studied. In the former the SmCo(1120) film shows a bicrystalline microstructure, whereas in the latter a uniaxial one is observed (figure 1). For the first time both microstructures were shown to consist of grains with a mixture of SmCo₃, Sm₂Co₇ and SmCo₅ polytypoids, i.e. compositionally stabilized structures observed only in high resolution images (figure 2). For such a microstructure we have proposed two alternative pinning mechanisms. The pinning sites could either be the incoherent twins observed at grain boundaries or the intragranular stacking disorders or SmCo polytypoids. Although Sm₂Co₇ has a high anisotropy, that of SmCo₅ is much higher and hence may impede the movement of domain walls.

To resolve such critical issues, it is important to be able to quantitatively image the domains, their interactions with microstructural features and their response to applied magnetic fields. We have recently developed and implemented a technique using a series of Lorentz images obtained at various beam tilts and subsequent processing to obtain quantitative vector plots of the in-plane induction. The objective lens fields have also been accurately measured making it possible to apply well defined fields in situ in the microscope to observe domain motion and pinning mechanisms. A representative image from a complicated ripple structure in FeCo alloys, illustrating this development, is shown in figure 3.

Contact: Kannan M. Krishnan, Lawrence Berkeley National Laboratory
Phone: (510) 486-4614 Fax: (510) 486-5888 E-mail: Kannan_Krishnan@macmail.lbl.gov

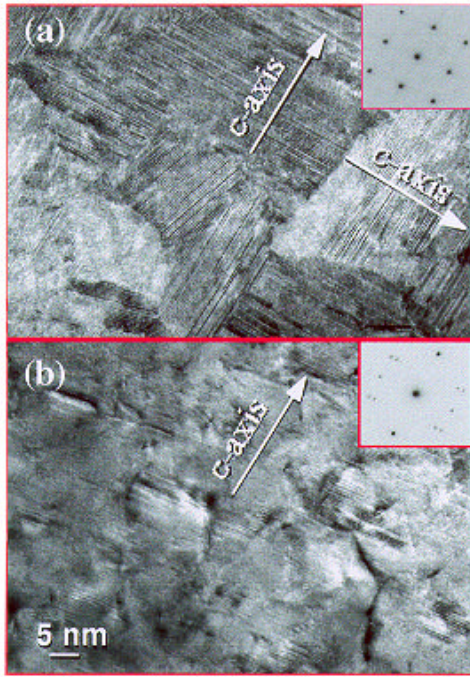


Figure 1. Low magnification HRTEM images showing the microstructure of the as-grown (a) SmCo(1120) and SmCo(1100) thin films. The respective electron diffraction is shown in insets.

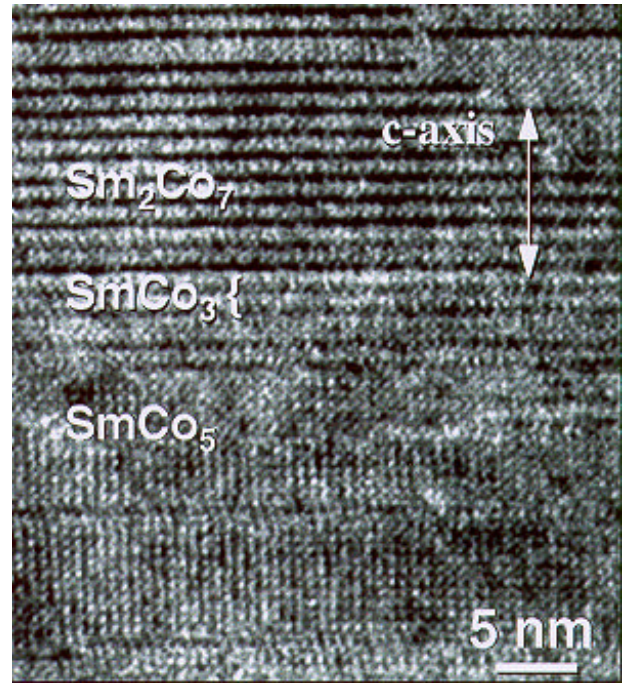


Figure 2. HRTEM image of a grain indicating the stacking disorder or formation of polytypoids along the c-axis.

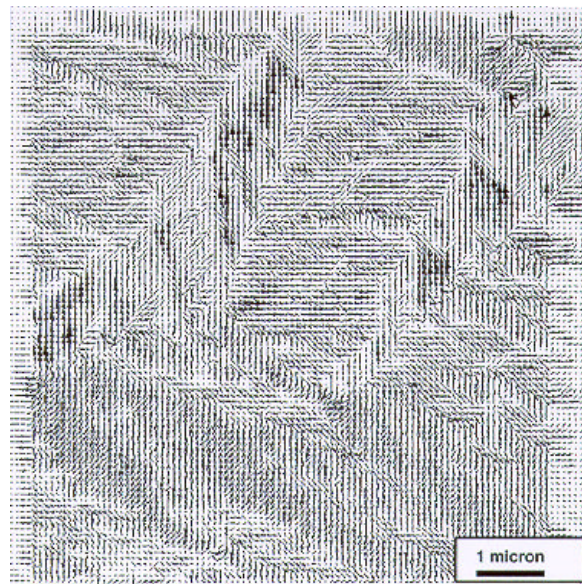


Figure 3. Vector representation of the in-plane induction of a ripple structure in Fe-Co alloy thin film. This plot is the result of processing a series of Lorentz images obtained with different tilts of the incident beam.

Light-Induced Metastability in Hydrogenated Amorphous Silicon

H. M. Branz, *National Renewable Energy Laboratory*

R. Biswas, *Ames Laboratory*

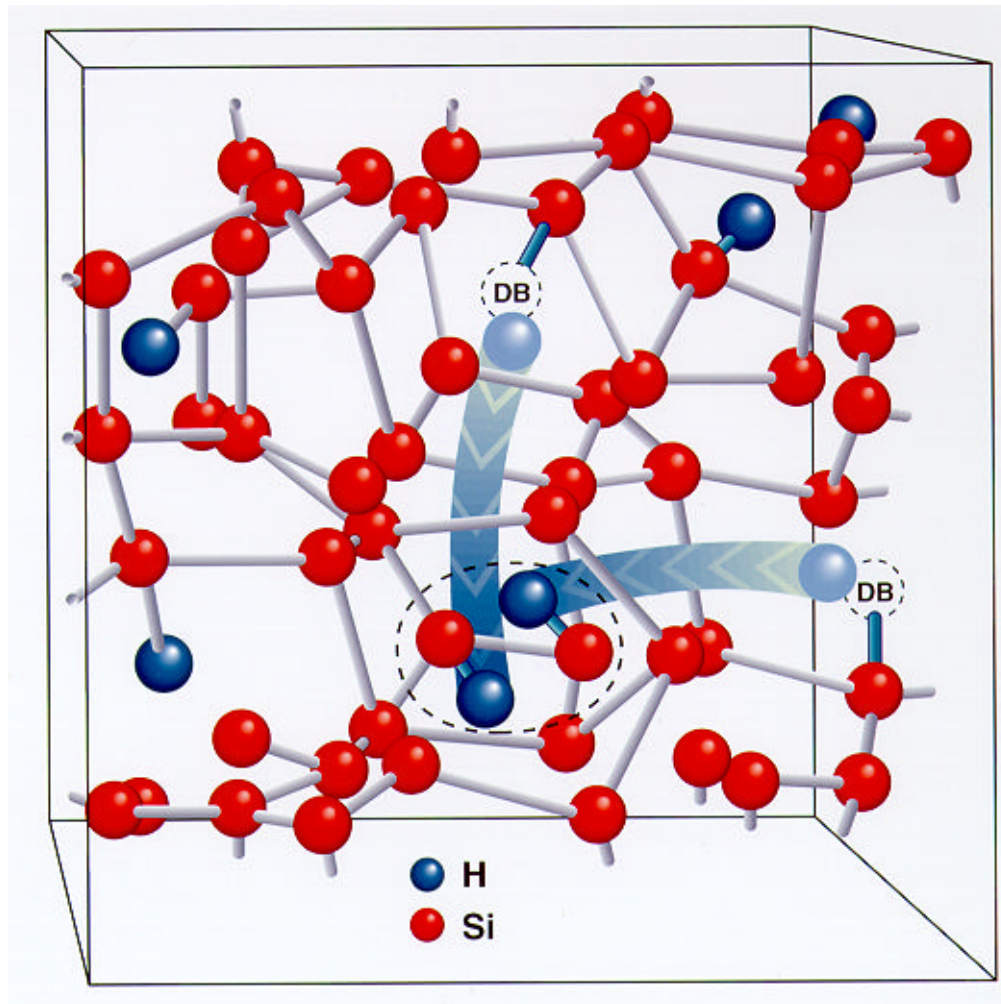
Motivation Light-induced metastability in hydrogenated amorphous silicon (a-Si:H), which limits solar cell performance, has been an important unsolved problem in amorphous silicon research since its discovery by Staebler and Wronski (SW effect) in 1977. Briefly, exposure of device quality a-Si:H to light increases the density of neutral dangling-bond (DB) defects by one to two orders of magnitude. The light-induced DBs are metastable and can be thermally annealed. There are strong indications that hydrogen is connected to the degradation effect. However, 20 years of extensive study has not produced a viable model for this defect formation, and this has undoubtedly contributed to an inability to eliminate this degradation phenomenon in a-Si:H solar cells. There remains a strong need for fundamental understanding of the microscopic nature of the formation of such defects in amorphous silicon.

Accomplishment A new model of light-induced metastability in a-Si:H has been proposed by one of us (Branz). According to this model, when two mobile hydrogen atoms created by light-induced carriers collide, they form a metastable immobile complex containing two Si-H bonds. Excess metastable dangling bonds remain at the uncorrelated sites from which the colliding H atoms were excited. The model accounts quantitatively for the kinetics of light-induced defect creation, both at near room

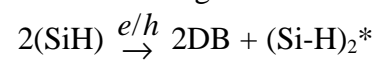
temperature and at 4.2K. Other experimental results, including light-inducing and thermal-annealing kinetics, are also explained. Branz's model predicts the formation of two hydrogen metastable complexes, but does not specify the exact microscopic configuration of these complexes. Biswas followed up this prediction with a theoretical computation of the total energies of a variety of two-H complexes in a-Si:H using molecular dynamic simulations. He found several configurations that meet the requirement of the model, including an analog of the H_2^* complex found in crystalline silicon (see figure).

Significance This model of the SW effect in amorphous silicon represents the first quantitative microscopic model to unify the great majority of experimental observations. This should inevitably lead to a better understanding of this complex phenomenon and enhance our ability to eliminate the degradation of a-Si:H solar cells. Once the light-induced metastability in amorphous silicon is eliminated, the efficiency of solar cells based on this material can be increased by at least 50%. This has enormous implications on the impact of this technology for large-scale photovoltaic applications. Besides technological impacts, this work should lead to some interesting scientific investigations to put the model on a stronger foundation.

Contact: Satyen Deb, National Renewable Energy Laboratory
Phone: (303) 384-6405 Fax: (303) 384-6481 E-mail: satyen_deb@nrel.gov



The figure shows a new model of light-induced metastability in a-Si:H:



Interfacial Microstructure in CdTe/CdS Heterojunction Solar Cells

Y. H. Kao, S. Huang, and Y. L. Soo, *SUNY, Buffalo, NY*
A. D. Compaan, *University of Toledo, Toledo, OH*

Motivation—The Thin film CdTe/CdS heterojunction solar cell has the potential to achieve very high efficiency (theoretical efficiency ~30%) at low-cost. Most recently a record 16% efficiency has been achieved using low-cost deposition techniques. Further improvement in performance efficiency requires fundamental understanding and control of various interfacial phenomena, such as roughness, potential fluctuations and diffusion, which control the charge transport and recombination kinetics. Synchrotron-radiation techniques of grazing incidence x-ray scattering and fluorescence provide powerful tools to investigate a variety of interfacial phenomena in this type of device.

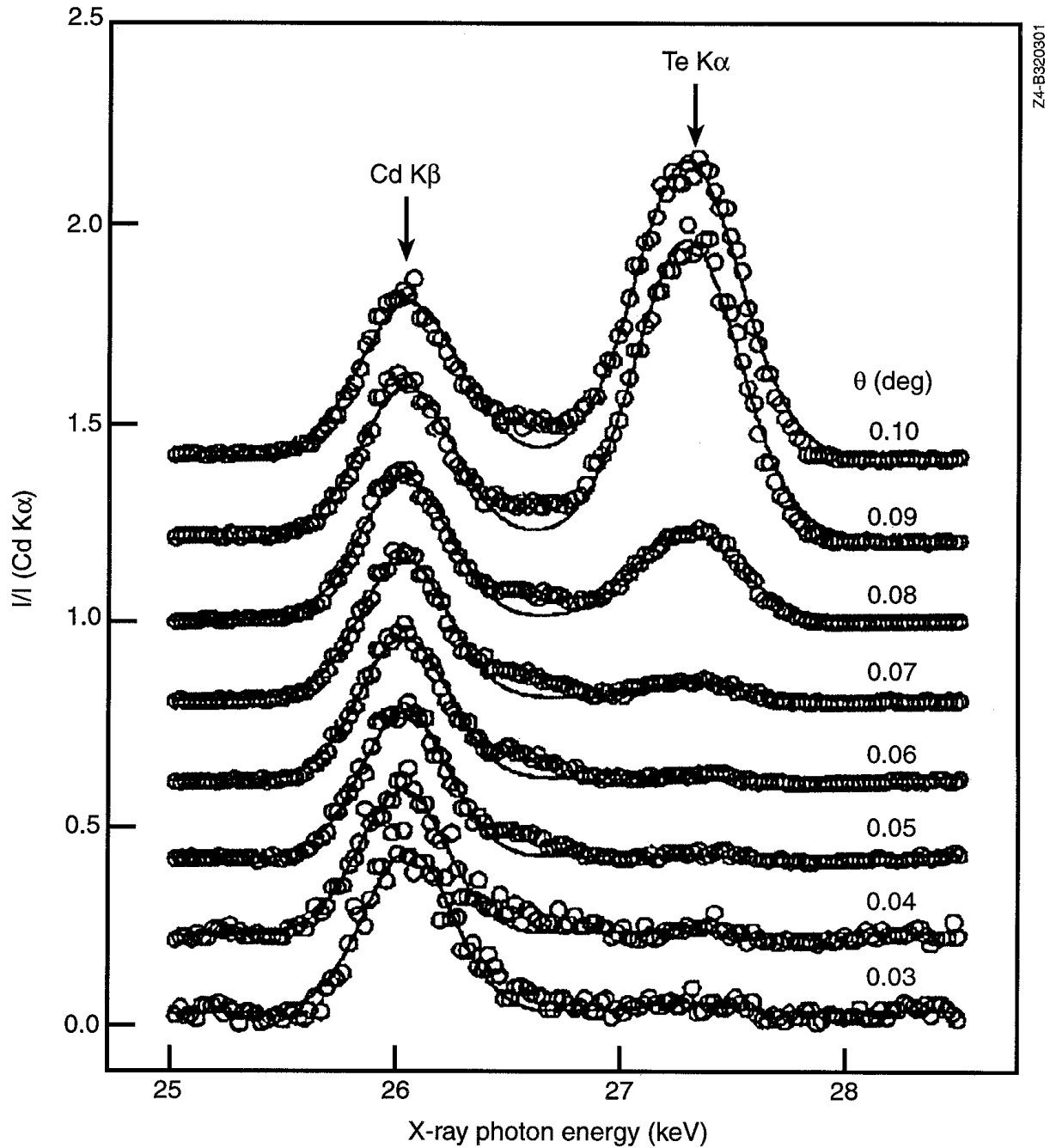
Accomplishment—Microscopic structure around the interfacial region between CdTe and CdS in CdTe/CdS heterojunctions has been investigated using x-rays from synchrotron radiation. These photovoltaic (PV) materials were prepared by RF sputtering onto Corning 7059 glass substrates and subjected to post-growth thermal annealing at different temperatures between 340 C and 385 C. A variety of x-ray techniques, including grazing incidence x-ray scattering (GIXS), angular dependence of x-ray fluorescence (ADXRF), anomalous x-ray scattering (AXS), and x-ray diffraction (XRD) have been employed to investigate the morphology around the interface region. From these measurements, the

interfacial roughness, correlation lengths of thickness fluctuations, Te density profile, and local environment surrounding specific atoms have been determined. The interfacial roughness between the sputtered films and Corning 7059 glass is found to be around 5 nm, and that between CdTe and CdS is around 20 nm as expected from the large (~10%) lattice mismatch. Special attention has been paid to the changes in Te density profile as a result of annealing. It has been found that by increasing the anneal temperature, the interfacial roughness increases and the correlation lengths are reduced. Te mixing between CdTe and CdS results in a more blurred interface.

Significance—The techniques used in this study offer very useful tools for non-destructive and element-specific characterization of the microstructure at the heterojunction and interfaces. The results show that heat treatment can cause significant mixing of Te between CdS and CdTe layers and the interface becomes more blurred. The extension of such studies on heterojunctions fabricated under different processing and annealing conditions can provide valuable insight into the role of interface microstructure on the optimization of device performance. Collaborative research efforts involving several laboratories, including NREL, are currently underway to study interfacial phenomena in a number of photovoltaic device structures.

Contact: Satyen Deb, National Renewable Energy Laboratory
Phone: (303) 384-6405 Fax: (303) 384-6481 E-mail: sateyn_deb@nrel.gov

Dependence of X-ray Fluorescence on θ



Typical data of angular dependence of x-ray fluorescence (ADXRF) for probing the density profile of Te in CdS/CdTe heterojunctions. The x-ray fluorescence yield of Te $K\alpha$ (fluorescence from the sample) varies sensitively with the grazing incidence angle θ which controls the penetration depth of incident x-rays.

Dopant Effects on Silicon Selective Nucleation and Solid Phase Epitaxy

H. A. Atwater, *California Institute of Technology*
 Tomas Diaz de la Rubia, *Lawrence Livermore National Laboratory*

Motivation Incorporation of electronic dopants (B, Al, P) into amorphous silicon at high concentration significantly enhances the solid phase epitaxy kinetics, but little is known about the basic mechanism for this phenomenon. What is known suggests that heavy doping does not fundamentally alter the atomic rearrangement event in crystallization, but it increases the density of sites for crystallization via an increased density of dopant-related defects (vacancy, dangling bond or other point defect). The goal of this project is to use a combined theoretical and experimental approach to elucidate the interactions of dopants, point defects and the amorphous-crystal interface in silicon in order to identify microscopic mechanisms underlying solid phase epitaxy. This understanding can be used to guide practical efforts to generate large-grain silicon microstructures for thin film photovoltaic applications.

Accomplishment When coupled with a site-selective heterogeneous nucleation process, solid phase crystallization can yield controlled microstructures with grain sizes exceeding 10 μm , as illustrated in Fig. 1. Experimental work has identified three regimes for the effects of dopants on solid phase epitaxy: i) below approximately $5 \times 10^{18}/\text{cm}^3$, none of the dopants studied have a significant effect on solid phase epitaxy; ii) between $5 \times 10^{18}/\text{cm}^3$ and some dopant-specific upper concentration bound, there is an increase in the solid phase epitaxy rate; and iii) above this upper bound, there is a decrease in the solid phase epitaxy rate, thought to be related to loss of dopant substitutionality, precipitation and segregation at the amorphous-crystal interface. These trends are summarized by the

data in Fig. 2. At high doping concentrations above $5 \times 10^{19}/\text{cm}^3$, a decrease in the incubation time for random crystallization has been found, suggesting heterogeneous nucleation related to dopant precipitation. Theoretical work using plane wave pseudopotential and tight binding molecular dynamics methods has focused on calculations of dopant-vacancy and dopant-dopant binding energies to determine whether vacancies and other point defects can play a role in solid phase epitaxy rate enhancement and heterogeneous nucleation at precipitated dopant clusters. To date, binding energies have been determined for neutral B-B pairs and B-interstitial defects to be 1.5 eV and 1.1 eV, respectively. The B-B pair was found to be electrically inactive. Calculations for B-vacancy defects, as well as for P defect complexes are underway.

Significance The finding of positive binding energy for electrically inactive B-B pairs is consistent with B precipitation and segregation at high concentration and loss of electrical activity. Both of these effects would contribute to a sublinear variation of solid phase epitaxy rate with B concentration at high concentrations. Also the electrically inactive B-B pairs may be a precursor to a heterogeneous nucleation site for random crystallization. A comprehensive correlation of solid phase epitaxy rate in regime (ii) with B-vacancy and P-vacancy binding energies will enable us to determine whether vacancies can play a role in solid phase crystallization. Moreover, knowledge of binding energies for large B and P clusters can be used to better understand dopant precipitation at high concentration, which is the ultimate limit to dopant-enhanced solid phase epitaxy of silicon.

Contact: H. Atwater, California Institute of Technology
 Phone: (818) 395-2197 Fax: (818) 395-7258 E-mail: haa@daedalus.caltech.edu

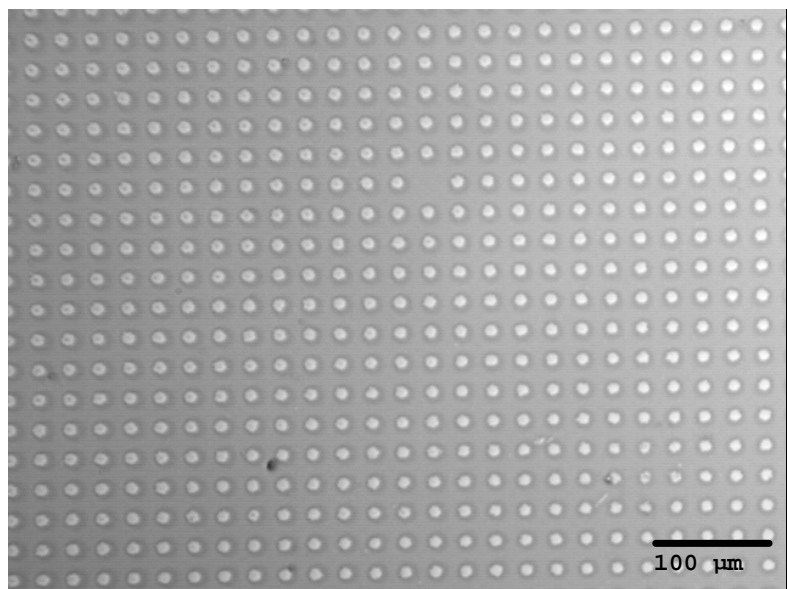


Fig. 1. Optical micrograph of 25 μm grid of selectively nucleated crystals in Al doped Si, with a peak concentration of $5.5 \times 10^{19}/\text{cm}^3$. Selective nucleation was achieved by metal induced nucleation, using 20 nm thick, 5 μm circles of In evaporated onto Si. Samples were vacuum anneal at 450°C for 20 min., followed by 600°C anneal for 3.5 hrs.

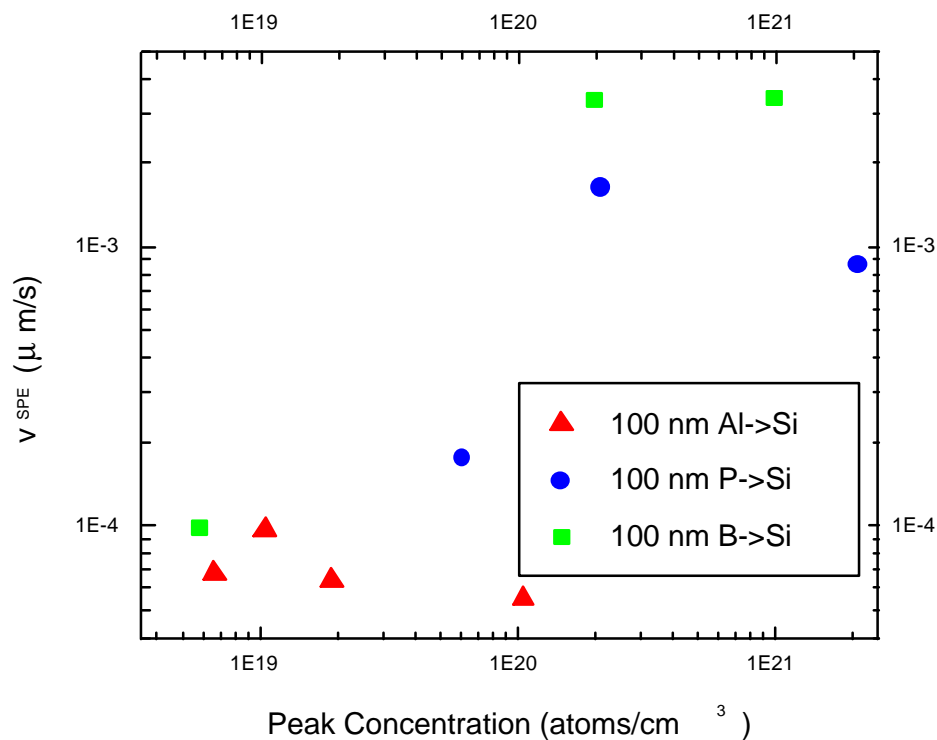


Fig. 2. Lateral solid phase crystallization rate at 620 °C for 100 nm thick doped Si layers vs. dopant peak concentration. Doping was achieved by ion implantation at a single energy.

Bonding Mechanism and Elastic Properties of Mo₅Si₃

C. L. Fu and Xindong Wang, *Oak Ridge National Laboratory*

MotivationThe attractive properties of transition-metal silicides for potential ultrahigh-temperature applications have been well recognized. Recent advances in the processing of materials have inspired a growing interest in Mo₅Si₃ based alloys. Unfortunately, these silicides are too brittle at ambient temperature to be used as structural engineering materials. At present, only limited scientific effort has been focused on understanding their brittle fracture behavior. For example, even the issue of the nature of interatomic bonding in these alloys is still not well understood. Furthermore, the physical basis for the high anisotropy in the coefficient of thermal expansion (CTE) generally observed for 5-3 transition-metal silicides is completely unknown. The anisotropy in CTE is viewed as a potentially detrimental factor concerning the microstructural compatibility in processing and application of these alloys.

AccomplishmentOur first-principles calculations provide understanding at an atomistic level of the intrinsic strength and thermoelastic behavior of binary Mo₅Si₃. The bonding is found to have pronounced multi-centered covalent components (Fig. 1), characterized by the planar Mo-Si-Mo triangular bonding units on the (001) plane and by the unusually short Mo-Mo bonds along the c-axis (shorter by about 10% relative to the Mo-Mo distance in the basal plane). These covalent bonds give rise to the strength of this material, and are manifest in a high heat of formation of -3.8 eV/formula unit for the T1 phase. While the calculated second-order elastic constants are consistent with the fact that the bonding in the (001) plane is stronger than the bonding along the [001] direction, the crystal anharmonicity is found to be higher along the [001] direction. (In other words, the lattice vibrational energy decreases more rapidly as the lattice is expanded

in the [001] direction than in the [100] direction.) A more elastically rigid (001) basal plane together with a higher anharmonicity along the c-axis contribute to a higher thermal expansion coefficient along the [001] direction than along the [100] direction (Fig. 2). The physical origin for the anisotropy in lattice anharmonicity lies in the dominant role of the unusually short [001] Mo-Mo covalent bonds in coupling the (001) layers. These multi-centered Mo-Mo bonds, that characterize the [100](001) shear, are weakened more by [001] expansions than by [100] expansions. Increasing [001] spacing reduces [001] Mo-Mo bond strength and decreases the lattice vibrational energy (giving higher lattice anharmonicity) more rapidly than in-plane expansions. This directional dependence of the Mo-Mo bond strength contributes significantly to the difference in the softening behavior of the [100](001) shear characteristics.

SignificanceUnderstanding the intrinsic mechanical behavior in this alloy requires a fundamental understanding of the electronic structure and bonding characteristics. In addition to providing understanding of the intrinsic high mechanical strength in terms of the existence of pronounced multi-centered covalent bonds, our theory also points out that the origin of thermal expansion anisotropy lies in the anisotropy of lattice anharmonicity. Our findings complement the experimental work at LANL and provide a valuable basis for future alloy design strategies. For example, we suggest that it is possible to reduce the anisotropy in CTE if the interlayer coupling of (001) layers is no longer dominated solely by the [001] bonding component. A modification of the bonding direction can most likely be achieved by interstitial alloying additions.

Contact: C. L. Fu, Oak Ridge National Laboratory
Phone: (423) 574-5161 Fax: (423) 574-7659 E-mail: fucl@ornl.gov

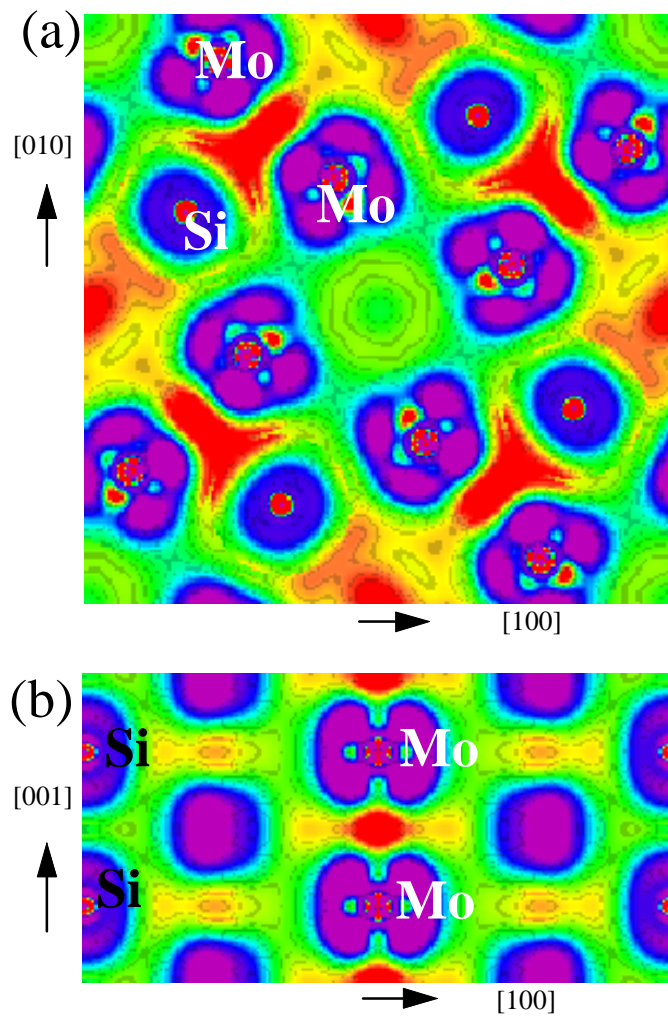


Figure 1. The calculated bonding charge density shows the depletion of density at the lattice sites (denoted by purple color) together with an increase of density in the interstitial region. The bonding has pronounced covalent components (emphasized by red color), characterized by (a) the planar Mo-Si-Mo triangular bonding units on the (001) plane, and by (b) the unusually short Mo-Mo bond along the c-axis. The increased charge density (referred to the overlapping atomic charge density) in the red colored regions has values larger than $1 \times 10^{-2} e / (\text{a.u.})^3$. These covalent bonds give rise to the strength of this alloy.

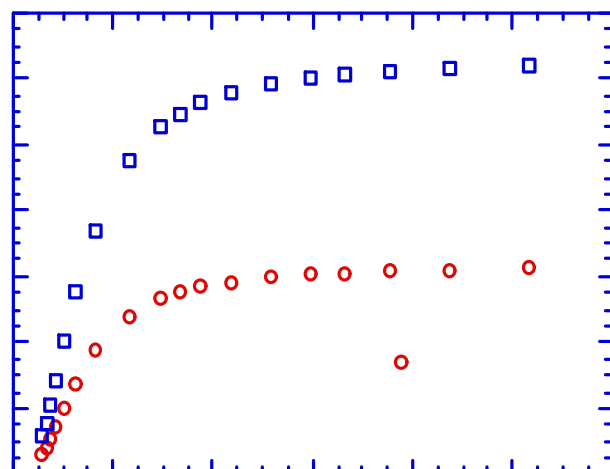


Figure 2. The calculated coefficient of thermal expansion (CTE) is highly anisotropic along the [001] and [100] directions

Superplastic Formability of Advanced Silicides

T. G. Nieh, L. Hsiung, and J. G. Wang, *Lawrence Livermore National Laboratory*

Motivation Despite its high temperature strength, Mo_3Si_5 is very brittle at room temperature and its ductile to brittle transition is relatively high ($>1000^\circ\text{C}$). Forming, shaping, and machining of Mo_3Si_5 are expected to be difficult, resulting from its high hardness and low toughness. Superplastic forming technology, which is a viable net-shape forming process, is thus especially attractive. The availability of superplastic forming technology would offer a niche to precision form advanced silicides into complex components which can be used efficiently for energy conversion.

Accomplishment The characterization of the nature of dislocations is essential to the understanding of high-temperature plasticity. We obtained several single crystals and polycrystals of Mo_5Si_3 from LANL. In the case of single crystals, microstructure was examined using transmission electron microscopy. No dislocations could be found in the as-grown single crystal as well as in a sample crept at 3 MPa and 1200°C . Both samples

exhibit extensive bend contour suggesting the existence of large internal stresses. This result is consistent with electric resistance measurements, which indicated that the as-grown Mo_5Si_3 single crystal is defect-free. In the case of polycrystals, X-ray diffraction analysis indicates the as-cast alloy is actually two-phase (Figure 1), presumably caused by chemical inhomogeneity. The microstructure of a sample creep deformed at 3 MPa and 1500°C is shown in Figure 2. Dislocations do appear in some grains. However, phase analysis indicates that dislocations are present only in the Mo_3Si grains. The Mo_5Si_3 grains in the arc-cast polycrystal are, in fact, still dislocation free. The characterization of the nature of these dislocations is underway.

Significance Results from the present investigation indicate that Mo_5Si_3 single crystals is very strong even at elevated temperatures ($\sim 1500^\circ\text{C}$). To promote plasticity in Mo_5Si_3 , the addition of a second soft phase appears to be necessary.

Contact: T. G. Nieh, Lawrence Livermore National Laboratory
Phone: (510) 423-9802 Fax: (510) 423-8034 E-mail: nieh1@llnl.gov

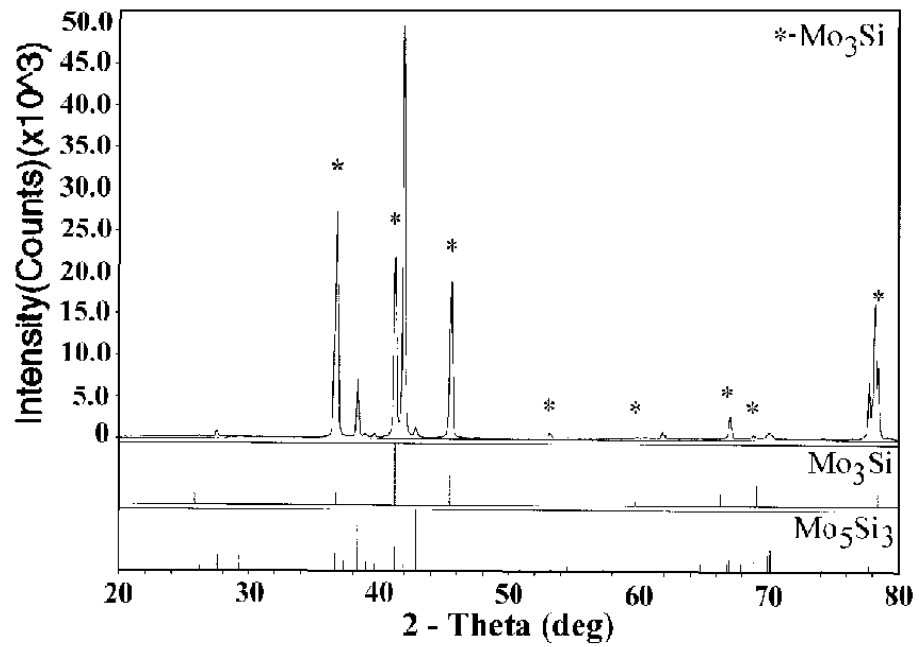


Figure 1. X-ray diffraction from an arc-cast polycrystalline silicide.

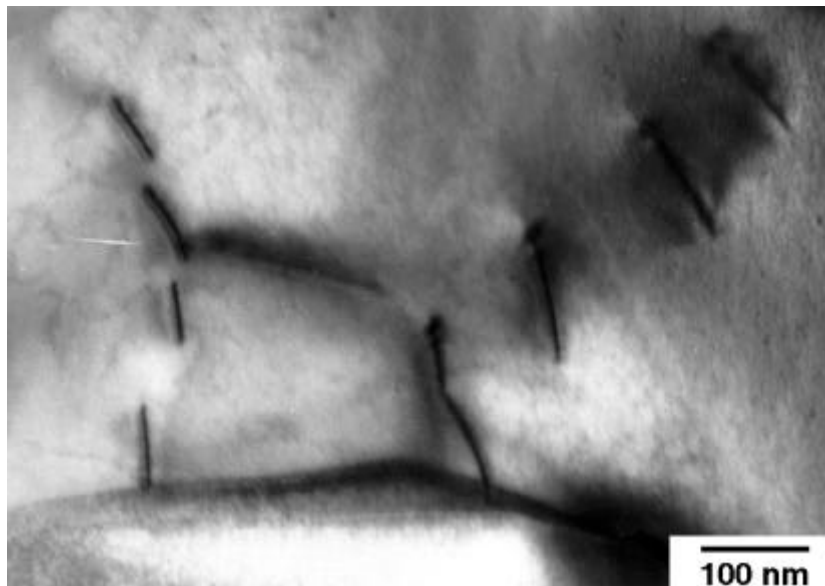
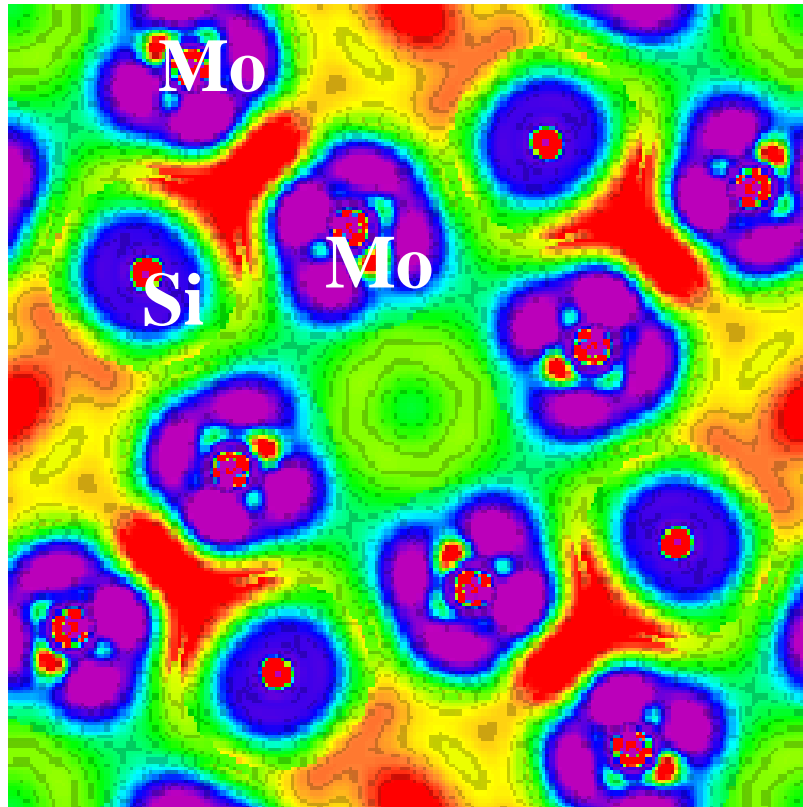


Figure 2. Microstructure showing the presence of dislocations in a Mo₃Si grain



The figures on the front and back covers relate to some of the accomplishments described in this issue of Research Briefs. The above figure shows results of first-principles calculation of the charge density at the lattice sites of Mo_5Si_3 showing the pronounced covalent bonding (red colored regions) which is responsible for the high strength of this ultrahigh-temperature intermetallic compound. The figure on the front cover shows stress distribution during nanoindentation of a multilayer diamond-like carbon film. Nanoindentation measurements combined with finite element modeling allow separation of the mechanical properties of the thin film from those of the substrate.

SAND98-0839: Prepared by the DOE Center of Excellence for the Synthesis and Processing of Advanced Materials at Sandia National Laboratories, Albuquerque, New Mexico 87185 for the Division of Materials Sciences, Office of Basic Energy Sciences, U.S. Department of Energy. Sandia is a multiprogram laboratory operated by Sandia Corporation, a Lockheed Martin Company, for the Department of Energy under Contract No. DE-AC04-94AL85000.

Printed in February 1998